Rapid Colorimetric Method Development for Detection of Fumonisins in Corn samples

Thaksinan Chotchuang

A Thesis Submitted in Partial Fulfillment of the Requirements for the Degree of Master of Science in Chemistry (Analytical Chemistry)
Prince of Songkla University
2019

Thesis Title	Rapid colorimetric method development for detection of fumonisins in corn samples
Author	Miss Thaksinan Chotchuang
Major Program	Chemistry (Analytical Chemistry)

Major Advisor	**Examining Committee :**
……..……	……....Chairperson
(Asst. Prof. Dr.Thitima Rujiralai)	(Asst. Prof. Dr. Supaporn Sangsrichan)
	……..…Committee
Co-advisor	(Dr. Panwadee Wattanasin)
……...…	……..…Committee
(Asst. Prof. Dr.Wilairat Cheewasedtham)	(Asst. Prof. Dr. Thitima Rujiralai)
	……..…Committee
	(Asst. Prof. Dr. Wilairat Cheewasedtham)

The Graduate School, Prince of Songkla University, has approved this thesis as partial fulfillment of the requirements for the Master of Science Degree in Chemistry (Analytical Chemistry)

……
(Prof. Dr. Damrongsak Faroongsarng)

Dean of Graduate School

This is to certify that the work here submitted is the result of the candidate's own investigations. Due acknowledgement has been made of any assistance received.

……. Signature

(Asst. Prof. Dr. Thitima Rujiralai)

Major Advisor

……. Signature

(Miss Thaksinan Chotchuang)

Candidate

I hereby certify that this work has not been accepted in substance for any degree, and is not being currently submitted in candidature for any degree.

…… Signature

(Miss Thaksinan Chotchuang)

Candidate

ชื่อวิทยานิพนธ์ การพัฒนาวิธีการตรวจวัดสีที่รวดเร็วสำหรับตรวจวัดสารพิษฟูโมนิซินในตัวอย่างข้าวโพด

ผู้เขียน นางสาวทักษิณันต์ โชติช่วง

สาขาวิชา เคมี (เคมีวิเคราะห์)

ปีการศึกษา 2561

บทคัดย่อ

การพัฒนาวิธีการตรวจวัดสีที่มีประสิทธิภาพสูงสำหรับตรวจวัดสารพิษฟูโมนิซิน ชนิดบีหนึ่ง อาศัยสารไฮโดรไลซ์ฟูโมนิซิน ชนิดบีหนึ่ง เป็นตัวเหนี่ยวนำให้เกิดการรวมกลุ่มของอนุภาคนาโนทองที่เคลือบพื้นผิวด้วยซิสเตียมีน ซึ่งวิธีการตรวจวัดสีทำได้โดยการไฮโดรไลซ์ฟูโมนิซิน ชนิดบีหนึ่ง ภายใต้สภาวะเบส (พีเอส 9) ทำให้ได้สารไฮโดรไลซ์ฟูโมนิซิน ชนิดบีหนึ่ง ก่อนนำไปทำปฏิกิริยาการเกิดสีด้วยอนุภาคนาโนทองที่เคลือบพื้นผิวด้วยซิสเตียมีน การรวมกลุ่มของอนุภาคนาโนทองที่เคลือบพื้นผิวด้วยซิสเตียมีนเกิดจากกลุ่มเอมีนของซิสเตียมีนบนพื้นผิวอนุภาคนาโนทอง เกิดพันธะไฮโดรเจนกับกลุ่มไฮดรอกซิลของสารไฮโดรไลซ์ฟูโมนิซิน ชนิดบีหนึ่ง ทำให้สารละลายเปลี่ยนสีจากสีแดงเป็นสีน้ำเงินอมเทา ภายใต้สภาวะที่เหมาะสม วิธีที่พัฒนาขึ้นให้กราฟการเติมสารมาตรฐานซึ่งพล็อตระหว่างอัตราส่วนการดูดกลืนแสง (A_{645}/A_{520}) และความเข้มข้นของโมนิซิน ชนิดบีหนึ่ง มีความเป็นเส้นตรงอยู่ในช่วง 2.0 ถึง 8.0 ไมโครกรัมต่อกิโลกรัม ($y = 0.0966 x + 0.1244$, $R^2 = 0.9904$) ขีดจำกัดการตรวจวัดและขีดจำกัดการตรวจวัดเชิงปริมาณเท่ากับ 0.90 และ 2.74 ไมโครกรัมต่อกิโลกรัม ตามลำดับ นอกจากนี้ค่าร้อยละการได้กลับคืนที่ยอมรับได้อยู่ในช่วง 93.1 ถึง 99.3 โดยมีค่าเบี่ยงเบนมาตรฐานสัมพัทธ์ของความเที่ยงภายในวันเดียวกันและระหว่างวันน้อยกว่าร้อยละ 6.2 วิธีการตรวจวัดสีสำหรับตรวจวัดสารพิษฟูโมนิซิน ชนิดบีหนึ่ง สามารถทำได้ง่าย สังเกตสีได้อย่างรวดเร็วด้วยตาเปล่า มีความไววิเคราะห์และมีความเฉพาะเจาะจงสูงต่อฟูโมนิซิน ชนิดบีหนึ่ง เมื่อเทียบกับสารพิษตัวอื่น ๆในกลุ่มไมโคทอกซิน ได้แก่ อะฟลาทอกซิน ซีลาลีโนน ซิตรินิน และพาทูลิน นอกจากนี้วิธีที่พัฒนาขึ้นสามารถนำไปประยุกต์ใช้ในการตรวจหาปริมาณฟูโมนิซิน ชนิดบีหนึ่ง ในตัวอย่างข้าวโพดได้อย่างมีประสิทธิภาพ

Thesis Title Rapid Colorimetric Method Development for Detection of Fumonisins in Corn samples

Author Miss Thaksinan Chotchuang

Major Program Chemistry (Analytical Chemistry)

Academic Year 2018

ABSTRACT

A robust colorimetric detection of fumonisin B1 (FB1) based on hydrolyzed product induced aggregation of cysteamine functionalized gold nanoparticles (Cyst-AuNPs) was established. The colorimetric assay is performed by hydrolyzing the fumonisin B1 under basic condition (pH 9) to obtain hydrolyzed fumonisin B1 (HFB1) before aggregation with Cyst-AuNPs. The aggregation of Cyst-AuNPs was marked with a change in solution color (wine-red to blue-gray) due to the interaction of hydrogen bonds between -NH_2 groups of Cyst-AuNPs and -OH groups of HFB1. Under the optimum condition, a good linear standard addition curve in a range of 2.0-8.0 µg kg^{-1} FB1 was obtained from the plot of absorbance ratio (A_{645}/A_{520}) *versus* FB1 concentration ($y = 0.0966x + 0.1244$, $R^2 = 0.9904$). The limit of detection (LOD) and limit of quantification (LOQ) were 0.90 and 2.74 µg kg^{-1}, respectively. Additionally, acceptable recoveries ranged from 93.1 to 99.3% and excellent inter- and intra-assay precisions were achieved less than 6.2%. The Cyst-AuNPs colorimetric method for determination of FB1 was also simple, rapid visual results, high sensitivity and selectivity over other competitive mycotoxins including aflatoxin, zearalenone, citrinin and patulin. Moreover, our developed method was successfully applied and suitable for detection fumonisin B1 in real corn samples.

Acknowledgements

The successful completion of this thesis would be quite impossible without the help of many people. I wish to express my gratitude to those who have contributed to the completion of this thesis:

I would like to thank my advisor, Assistant Professor Dr. Thitima Rujiralai and my co-advisor, Assistant Professor Dr. Wilairat Cheewasedtham for giving me the opportunity to work on my interested field for their guidance, advice, encouragement, suggestions and support throughout the whole duration of this work.

I would like to thank the examining committee members, Assistant Professor Dr. Supaporn Sangsrichan and Dr. Panwadee Wattanasin, for their good comments and suggestions and their valuable time.

I would like to thank Professor Dr. Jens Christian Tjell for his great suggestion and guidance for thesis.

I would like to thank all instructors and all staff in the Department of Chemistry for my education and training throughout this graduate studies.

I would like to thank the Research Assistantship (Contract No. 1-2559-02-002), Faculty of Science, Prince of Songkla University, the Department of Chemistry, the Center of Excellence for Innovation in Chemistry (PERCH-CIC), and the Graduate School, Prince of Songkla University for the financial support during the research.

Thanks also go to the Department of Chemistry, Faculty of Science, Prince of Songkla University for the support of available facilities.

Many thanks go to all members in research room Ch315, members of graduate student and my best friends for continual care throughout this thesis.

Finally, and most importantly, I would like to thank my family for their loves, encouragement, understanding and support throughout my life.

Thaksinan Chotchuang

The Relevance of the Research Work to Thailand

The purpose of this Master of Science Thesis in Chemistry (Analytical Chemistry) is to develop the colorimetric method for detection of fumonisin B1 based on hydrolyzed product induced aggregation of cysteamine functionalized gold nanoparticles and to apply for determination of fumonisin B1 in corn samples.

The developed method is robust colorimetric sensor which is simplicity, rapid visual results, highly sensitive and selective for detection of fumonisin B1 in corn samples. This work can be an alternative method and applied to monitor the fumonisin B1 contaminated in corn samples as the screening test for food safety.

Contents

Contents (continued)

Contents (continued)

Contents (continued)

Contents (continued)

List of Tables

List of Figures

List of Figures (continued)

List of Figures (continued)

List of Abbreviations

AgNPs	Silver nanoparticles
AOAC	Association of Official Analytical Chemists
AuNPs	Gold nanoparticles
Cyst-AuNPs	Cysteamine capped gold nanoparticles
DAD	Diode array detector
ELEM	Equine leukoencephalomalacia
FB1	Fumonisin B1
FDA	The Food and Drug Administration
FLD	Fluorescence detector
HFB1	Hydrolyzed fumonisin B1
HLB	Hydrophilic-lipophilic balance
HPLC	High performance liquid chromatography
IARC	The International Agency for Research on Cancer
ICH	The International Council for Harmonization of Technical Requirements for Pharmaceuticals for Human Use
LOD	Limit of detection
LOQ	Limit of quantification
LSPR	Localized surface plasmon resonance
RSD	Relative standard deviation
SD	Standard deviation
SPE	Solid phase extraction
SPR	Surface plasmon resonance
TEM	Transmission electron microscopy
UV-Vis	Ultraviolet-Visible

CHAPTER 1

INTRODUCTION

1.1 Background and rationale

Mycotoxins are toxic secondary metabolites produced by filamentous fungi as *Fusarium, Aspergillus* and *Penicillium* species (Zöllner et al., 2006) that readily colonize crops in the field or after harvest. Examples of mycotoxins that cause illness in human and animal include aflatoxin, ochratoxin A, fumonisins, citrinin, patulin, zearalenone and trichothecenes. They were found to be contaminated in cereals, dried fruits, spices, coffee, juice, milk and dairy products. It has harmful effects for humans and animals. Some mycotoxins are carcinogenic while others are hepatotoxic, nephrotoxic, or immunosuppressive (Turner et al., 2009).

Fumonisins are the one group of mycotoxins produced principally by several *Fusarium* species, *i.e.*, *Fusarium verticilloides* and *Fusarium proliferatum* which is a worldwide contaminant of corn and corn products consumed by animals and humans (Li et al., 2012). Several fumonisin have been reported of which fumonisin B1 (FB1) is the most abundant naturally occurring in corn and highest toxic of fumonisins species followed by fumonisin B2 (FB2) and fumonisin B3 (FB3) (Ling et al., 2015; Ndube et al., 2011). It causes several diseases in animal and human, such as pulmonary edema in pigs, encephalomalacia in horses, and hepatic and renal toxicity in several species (Ling et al., 2015). Especially, fumonisin B1 is the most human health risk that causes aesophagal cancer in humans. The International Agency for Research on Cancer declared FB1 to be a group 2B carcinogen (possibly carcinogenic in humans) (IARC, 2000). Then, The Food and Drug Administration (FDA) has limited the maximum residues for FB1 in different foods, as 2-4 mg kg^{-1} total fumonisins (FB1 + FB2 + FB3) for human foods, and 5-100 mg kg^{-1} for animal feeds (Wang et al., 2012).

As the previous report, approximately 70% of the total detected fumonisins was fumonisin B1 which found in naturally contaminated samples, especially in corn samples (Ling et al., 2015). In addition, Thailand is an agricultural country. There are many kinds of plants grown. Particularly corn is the third most important economic crop of Thailand in terms of production and cultivation value, following rice and cassava (Yoshizawa et al., 1996). The presence of fumonisin B1was found in corn and corn products (Tansakul et al., 2013). Thus, we are considering of the toxicity and contamination of FB1. Furthermore, the determination of fumonisin B1 are important to control the quality of corn and corn products. The main purpose is to protect human and animal health from contamination of fumonisin B1 in corn and corn product.

Recently, several analytical methods have been used for detection fumonisin B1 in different samples, such as high performance liquid chromatography-fluorescence detection (Tangmunkhong et al., 2008; Yoshizawa et al., 1996; Yamashita et al., 2014), liquid chromatography-tandem mass spectrometry (Bryla et al., 2016; Gazzotti et al., 2009; Tansakul et al., 2013), electrochemical immunosensor (Kadir et al., 2010; Lu et al., 2016) and enzyme linked immunosorbent assay (ELISA) (Barna-Vetro et al., 2000; Sheng et al., 2012). Although these methods are high sensitivity and reliability but these approaches require expensive equipment and skilled analysts, time-consuming, and tedious steps. Therefore, the detection methods described above did not meet on-site testing. The earlier reports for fumonisin B1 detection used gold nanoparticles (AuNPs) labelled antibody (Ling et al., 2015). Their methods were high selectivity and sensitivity due to biological compatibility and unique physical. However, this method also has some drawback, including extra reagent requirement for stabilizing antibody and enzymes, and tedious labeling process.

Nowadays, the gold nanoparticles (AuNPs) are used widely due to its rapid, low cost and selective (Zhou et al., 2014). AuNPs sensor is used as colorimetric probes because of their distance-dependent optical properties, high extinction coefficients at visible region and ease of functionalization with organic ligands (Wang et al., 2013;

Zhou et al., 2014). The cysteamine functionalized AuNPs (Cyst-AuNPs) have been used as colorimetric sensor for detection of sulfate (Zhang et al., 2011), atrazine (Liu et al., 2016), aflatoxins (Sharma et al., 2010) and creatine kinase (Kumar et al., 2018). These analytes induced Cyst-AuNPs to aggregate *via* hydrogen bonding of amino groups of cysteamine on AuNPs surface (Liu et al., 2016; Zhang et al., 2011). Cyst-AuNPs was changed from dispersion to aggregation states which was based on their unique surface plasmon resonance, resulting in changes of the Cyst-AuNPs from red to blue. Based on this principle, colorimetric method was developed for the detection of fumonisin B1.

In this work, the colorimetric method based on aggregation of Cyst-AuNPs for determination of fumonisin B1 in corn was developed for the simple, sensitive, selective and reliable method. The procedure for measurement has 2 steps: fumonisin B1 is hydrolyzed by potassium hydroxide to obtain hydrolyzed fumonisin B1 (HFB1) and HFB1 induced Cyst-AuNPs to aggregate through the hydrogen bonding. The aggregation of Cyst-AuNPs results color change from wine red to blue gray and corresponding absorption spectra change from 520 nm to 645 nm. This method was applied in corn samples that can be easily observed by naked eyes, and also measured by UV-Vis spectrophotometer.

1.2 Review of literature

1.2.1 Fumonisin B1

Fumonisin B1 (FB1) is the diester of propane-1,2,3-tricarboxylic acid and a pentahydroxyeicosane in which the C14 and C15 hydroxy groups are esterified with the terminal carboxy group of propane-1,2,3-tricarboxylic acid (TCA). The molecular formula of FB1 is $C_{34}H_{59}NO_{15}$ and molecular weight is 721.84 g mol^{-1} (Yazar & Omurtag, 2008) as shown in Figure 1.1.

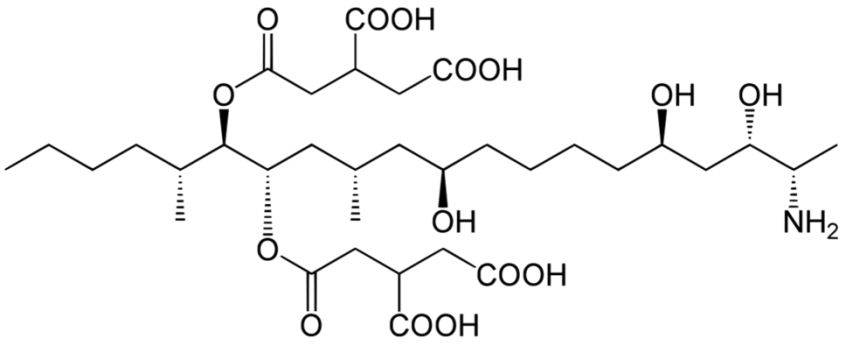

Figure 1.1 The chemical structure of fumonisin B1.

Fumonisin B1 is toxins which in a group of fumonisins. It was produced by several species of *Fusarium* molds such as *Fusarium verticilloides* and *Fusarium proliferatum* which occur in corn, wheat and other cereals (Li et al., 2012). Temperature and moisture conditions are crucial factors affecting fungal infection and toxin synthesis (Yazar & Omurtag, 2008). Fumonisin B1 is the most abundant naturally and highest toxic followed by fumonisin B2 (FB2) and fumonisin B3 (FB3). It was contaminated in mainly corn and corn products consumed by animals and humans (Ling et al., 2015).

Fumonisin B1 is white hygroscopic powder and can dissolve in many solvents such as water which soluble at least to 20 g L^{-1}, methanol and acetonitrile-water (IARC,2000). Stability of fumonisin B1 is stable in acetonitrile-water (1:1) at 25˚C (Gelderblom et al., 1992) and in methanol at -18˚C (Visconti et al., 1994).

Toxicity of fumonisin B1 has been reported that fumonisin B1 causes equine leukoencephalomalacia (ELEM), porcine pulmonary oedema syndrome and promote tumor in rat. Especially, fumonisin B1 also cause neural tube defects during the first month of pregnancy and human oesophagal cancer (Voss et al., 2007). Accordingly, the International Agency for Research on Cancer declared fumonisin B1 to be a group 2B carcinogen (possibly carcinogenic in humans) (IARC, 2000). Moreover, the Food and Drug Administration (FDA) recommended maximum levels for total fumonisins

(FB1, FB2 and FB3) in corn and corn products for human food (NGFA U.S., 2011) as shown in Table 1.1.

Table 1.1 FDA guidance levels of fumonisin for corn and corn products intended for human food.

Product	**Total Fumonisins (FB1, FB2 and FB3)** [parts per million: ppm]
Degermed dry milled corn products (e.g., flaking grits, corn grits, corn meal, corn flour with fat content of < 2.25%, dry weight basis)	2
Whole or partially degermed dry milled corn products (e.g., flaking grits, corn grits, corn meal, corn flour with fat content of ≥ 2.25 %, dry weight basis)	4
Dry milled corn bran	4
Cleaned corn intended for masa production	4
Cleaned corn intended for popcorn	3

Thakur et al. (1996) reported the changing of fumonisin B1 structure *via* hydrolyzed process with alkaline media. Fumonisin B1 is a large molecule and contains tricarboxylic acid side chains which probably cause sterilization. Therefore, the method previously mentioned have been used to hydrolyze the structure of fumonisin B1 to be smaller through replacement of tricarballylic acid side chains by hydroxyl groups as shown in Figure 1.2.

Finally, the structure of hydrolyzed fumonisin B1 that contains several hydroxyl groups and an aliphatic amine group are expected to be able to interact with developed probe.

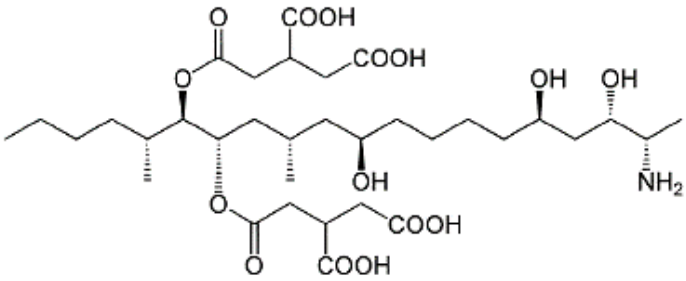

Fumonisin B1 – (MW 721.84 g mol^{-1})

Alkaline hydrolysis

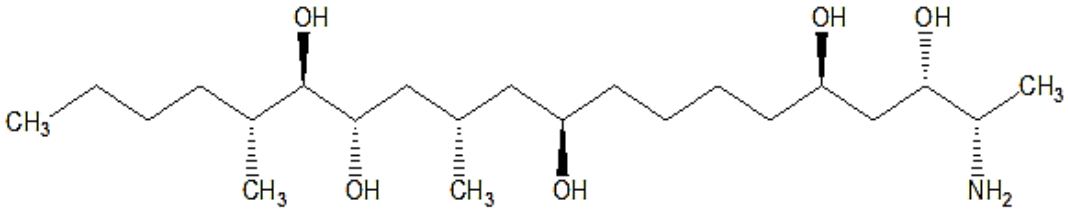

Hydrolyzed fumonisin B1 – (MW 405.61 g mol^{-1})

Figure 1.2 Chemical structures of the fumonisin B1 and hydrolyzed fumonisin B1.

1.2.2 Gold nanoparticles (AuNPs)

1.2.2.1 Introduction of gold nanoparticles

Nowadays, gold nanoparticles (AuNPs) and silver nanoparticles (AgNPs) are increasing applied to detect many compounds and used in many products such as cosmetics, detergents and paints (Rashid et al., 2014). The benefits of addition of AuNPs and AgNPs into products that come from the special and useful properties of nanoparticles are, for example, antibacterial, and self-cleaning (Sharma et al., 2009). In addition to these capabilities, AuNPs and AgNPs also exhibit other interesting properties which have potentials to be employed in many applications such as sensing in biosensor.

The advancement of nanotechnology and nanoscience has opened up new opportunities for the application of nanomaterials in biosensor. Noble metal nanoparticles, such as gold (Au) and silver (Ag) have received great interest due to the unique structural and photophysical features of nanomaterials (Zhang et al., 2011). Especially, gold nanoparticles (AuNPs) are widely used as optical nanoprobes for sensitive detection owing to localized surface plasmon resonance phenomena (LSPR) (Kong et al., 2016).

Gold nanoparticles (AuNPs) are small gold particles with a diameter of 1 to 100 nm which, once dispersed in water, are also known as colloidal gold. AuNPs have unique surface, magnetically properties, high electron density, strong optical absorption and unique optical properties which are largely dependent on the size, shape, and most importantly their inter-particle distance (Rashid et al., 2014). Their unique property of tune-able localized surface plasmon resonance (LSPR) absorption offers rapid visual results and simplicity for on-site investigation (Sabela et al., 2017).

1.2.2.2 The surface plasmon resonance phenomenon

The photonics properties of AuNPs are mainly the results of the electromagnetic induced phenomenon called localized surface plasmon resonance (LSPR), which is originated from the coherent oscillations of the conductive electrons at the surfaces of AuNPs upon excitation (illumination) of electromagnetic field (light). Illustration of LSPR of a AuNPs upon excitation of an electromagnetic filed (light) is shown in Figure 1.3 (Swanglap, 2016).

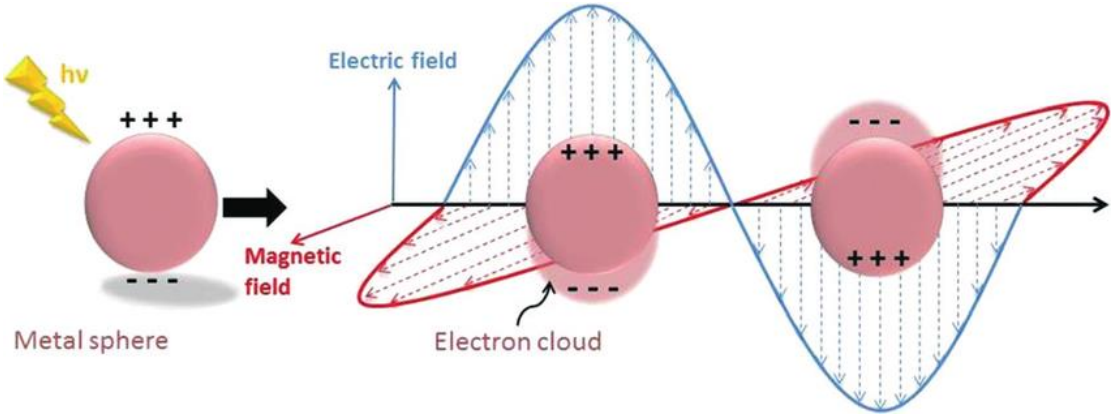

Figure 1.3 Schematic description of localized surface plasmon resonance in metal nanoparticles (Peiris et al., 2015).

LSPR is unique to metal type, shape, and size of metal nanoparticles (Willets et al., 2007). For AuNPs, LSPR are mainly in visible wavelengths (400-800 nm), and can even be measured to UV and near IR wavelength by controlling theirs shapes and sizes with specific synthesis conditions (Freitas et al., 2018). For example, small (~30 nm) monodisperse AuNPs, LSPR causes an absorption of light in the blue-green portion of the spectrum (~450 nm) while red light (~700 nm) is reflected, yielding a rich red color. As particle size increases, the wavelength of surface plasmon resonance related absorption shifts to longer, redder wavelengths. Red light is then absorbed, and blue light is reflected, presenting solutions with pale blue or purple color (Swanglap, 2016).

These specific absorptions of the AuNPs via their LSPRs are reflected as the different colors of AuNPs in the solution phases as shown in Figure 1.4.

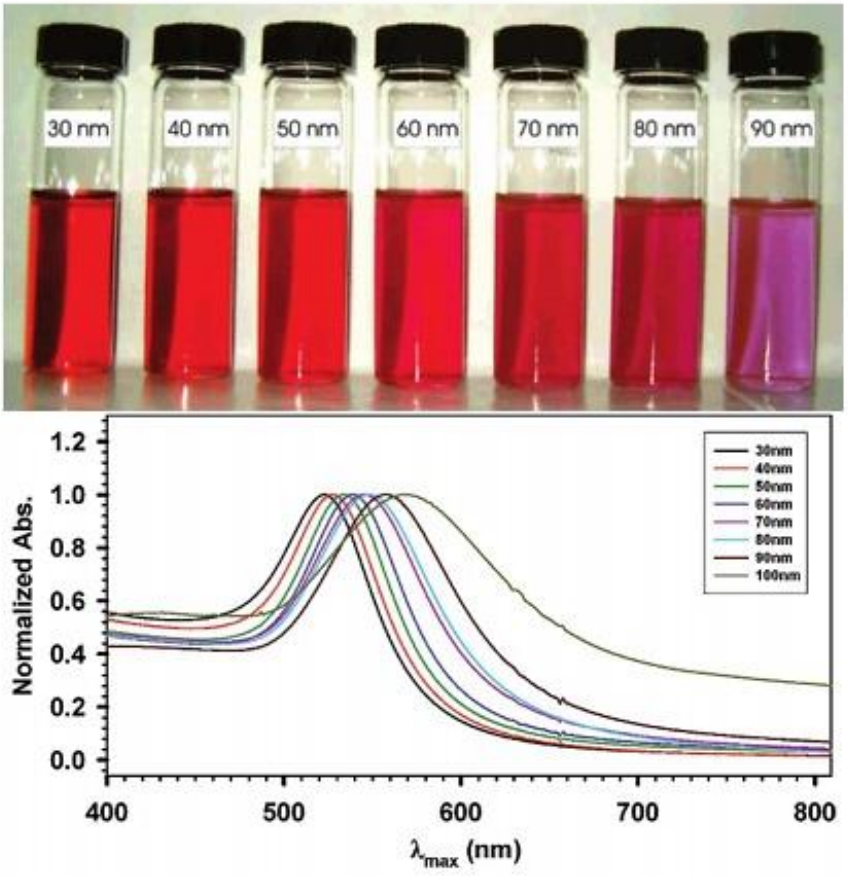

Figure 1. 4 Colors of AuNPs at different particle sizes after reduction with reducing agent and unique LSPR of different AuNPs sizes in the UV-Vis spectra (Subara & Jaswir, 2018).

1.2.2.3 The synthesis method of AuNPs

The most widely utilized chemical method is the Turkevich- Frens citrate reduction of gold (III) derivative method. The particle size of AuNPs synthesized by this method was between 10 to 100 nm. The method is satisfactory due to its simplicity, controllable size and stable colloidal nanoparticles produced (Ajdari et al., 2017).

Today, this method is often used and modified to contain other ligands with specific functions.

In the Turkevich-Frens method, $HAuCl_4$ is used as a precursor. The $HAuCl_4$ solution was vigorous boiled, then sodium citrate solution (reducing agent) were injected to the boiling solution under vigorous boiling and stirring. Citrate was reduced and stabilized the AuNPs from aggregation. The AuNPs are collected after the appearance of a wine-red colloidal solution is observed (Subara et al., 2018). The reduction of $HAuCl_4$ was carried out by sodium citrate, in which Au^{3+} was reduced to Au^0 atom. The gold atoms will form dimers and small clusters. Then, the clusters grow due to aggregation and coalescence until reaching a final particle size at which the particles are sufficiently stabilized as shown in Figure 1.5 (Polte, 2015). As this procedure is reasonably simple and environmentally friendly, it is the most commonly used method for the synthesis of AuNPs.

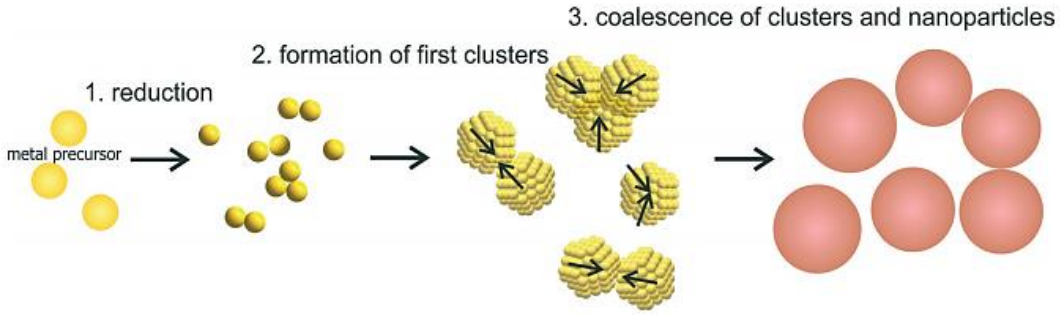

Figure 1.5 The growth mechanism of metal nanoparticles with Turkevich-Frens method (Polte, 2015).

1.2.2.4 The application to colorimetric sensing based on AuNPs aggregation

AuNPs is a nanomaterial that has been widely used in high technology applications such as sensory probes, electronic conductors, therapeutic agents, organic photovoltaics, drug delivery in biological and medical applications, and catalysis (AZoNano, 2013). Due to their unique optical properties, AuNPs was applied to colorimetric sensor for detection of hazardous chemicals, such as pesticide residues, heavy metals, banned additives, and biotoxins, in food as shown in Figure 1.6 (Liu et al., 2018).

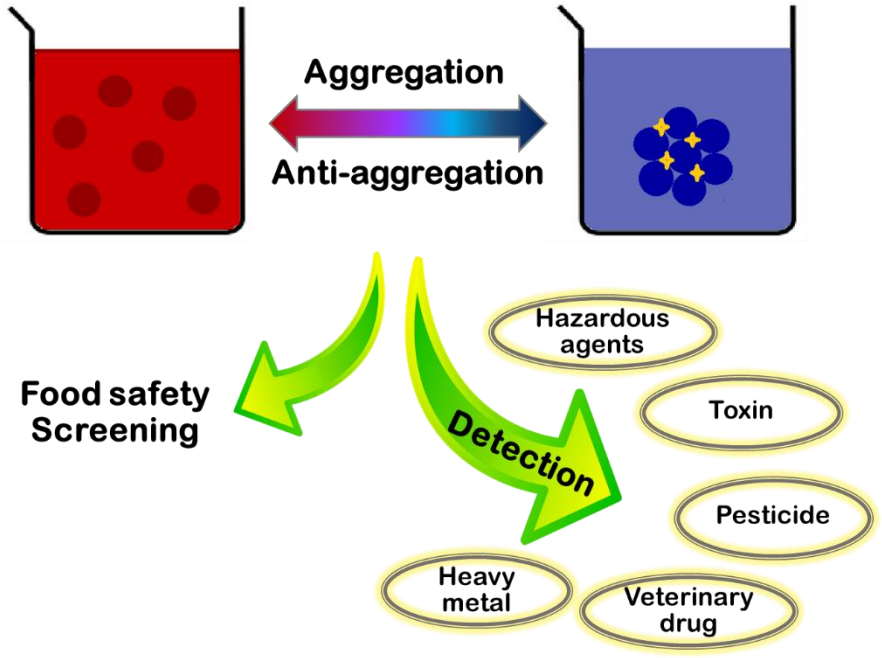

Figure 1.6 Application of gold nanoparticle colorimetric sensors (Modified from Liu et al., 2018).

Moreover, the trend of the AuNPs- based colorimetric sensor is increased continuously because it is simple, fast, low cost and sensitive. This method is used extensively in real-time on-site monitoring and rapid testing of food quality and safety (Liu et al., 2018).

In past few years, cysteamine has been used as stabilizer and modifier which can be functionalized on the AuNPs surface. Since cysteamine has the thiol group, thus it easily modifies on surface of AuNPs through Au-S covalent bond. The colorimetric sensing of modified AuNPs occurs when analyte induces modified AuNPs to aggregate and decreases the stability of modified AuNPs. Thus, color of AuNPs changes from red to blue (Zhang et al., 2011). Figure 1. 7 is an example of colorimetric sensing mechanism for atrazine based on aggregation of cysteamine functionalized AuNPs (Liu et al., 2016).

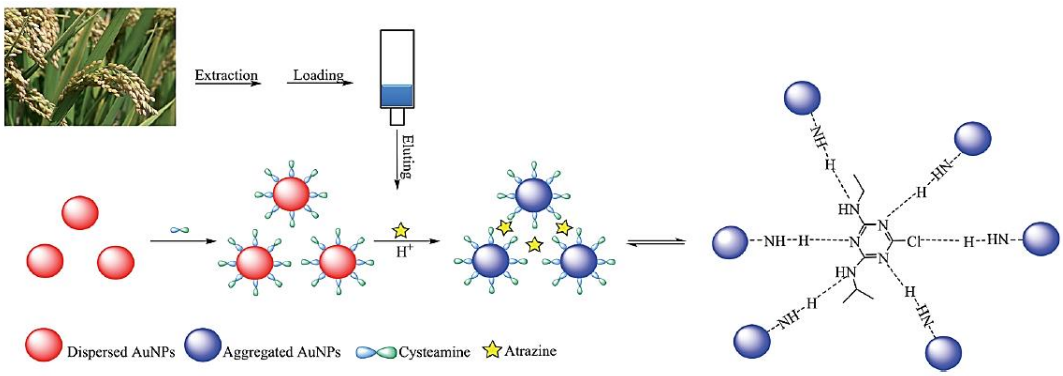

Figure 1. 7 The schematic of colorimetric sensing of atrazine in rice samples using cysteamine functionalized gold nanoparticles (Liu et al., 2016).

In addition, example of cysteamine modified on gold nanoparticles surface which are based on the electrostatic attraction for melamine and the N–Hg–N structure for Hg^{2+} was reported by Ma et al. (2013) as shown in Figure 1.8.

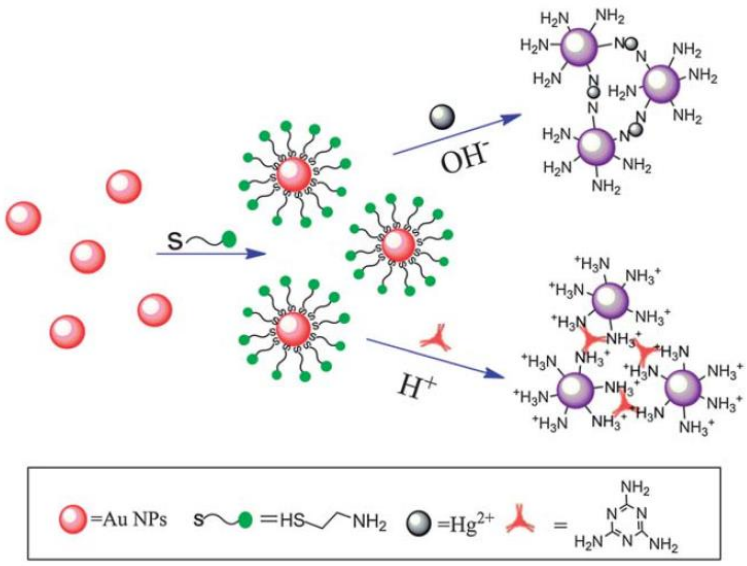

Figure 1.8 Schematic of the colorimetric detection strategy for Hg^{2+} and melamine based on cysteamine modified AuNPs (Ma et al., 2013).

Furthermore, several previous reports mentioned the degradation of the analyte structure before reacting with modified AuNPs to increase the specificity of the sensor (Akhond et al., 2015). Figure 1.9 is an example of the colorimetric method for detection of degradation of amoxicillin based on induced aggregation of gold nanoparticles. Amoxicillin was degraded to penicillamine by hydrolysis in acidic media. When penicillamine was added, the color of citrate capped AuNPs changed from red to blue due to formation of intermolecular H-bonds with incoming ligand.

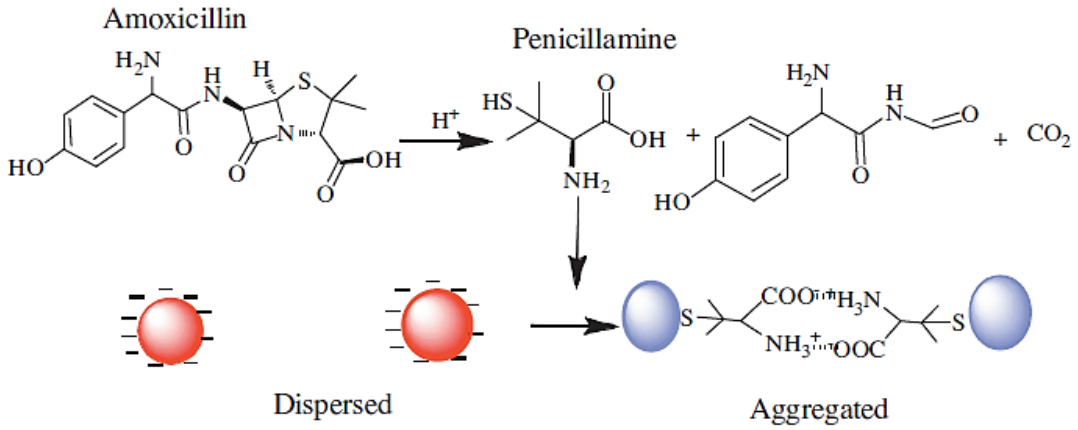

Figure 1.9 The schematic representation of degradation of amoxicillin in acidic media and its induced aggregation on citrate-capped gold nanoparticles (Akhond et al., 2015).

1.2.3 Analytical techniques

1.2.3.1 Ultraviolet-Visible spectrophotometry

UV-Vis spectroscopy is routinely used in analytical chemistry for the qualitative and quantitative determination of different analytes in solution as well as solids and gases. The ultraviolet region falls in the range between 190 to 400 nm whereas the visible region ranged between 400 to 800 nm. The Beer-Lambert's law states that the absorbance of a solution is directly proportional to the concentration of the absorbing species in the solution and the path length. Thus, for a fixed path length, UV-Vis spectroscopy can be used to determine the concentration of the absorber in a solution by observing the absorbance change with concentration. Moreover, UV-Vis spectrophotometry was applied for nanomaterial technology because of colorimetric properties of gold nanoparticles.

The example of a schematic diagram of a UV-Vis spectrophotometer is shown in Figure 1.10. The light source (a combination of tungsten/halogen and deuterium lamps) provides the visible and near ultraviolet radiation covering the 200-800 nm. The

output from the light source is focused onto the diffraction grating or prism which can devide the incoming light into its component colors of different wavelengths. For liquids, the sample cell is held in an optically flat, transparent container called a cell or cuvette. The reference cell or cuvette contains the solvent in which the sample is dissolved and this is commonly referred to as the blank. The detector converts the incoming light into signal like, current or voltage which the higher the current the greater the intensity. The computer or chart recorder usually plots the absorbance against wavelength (nm) in the UV and visible section of the electromagnetic spectrum.

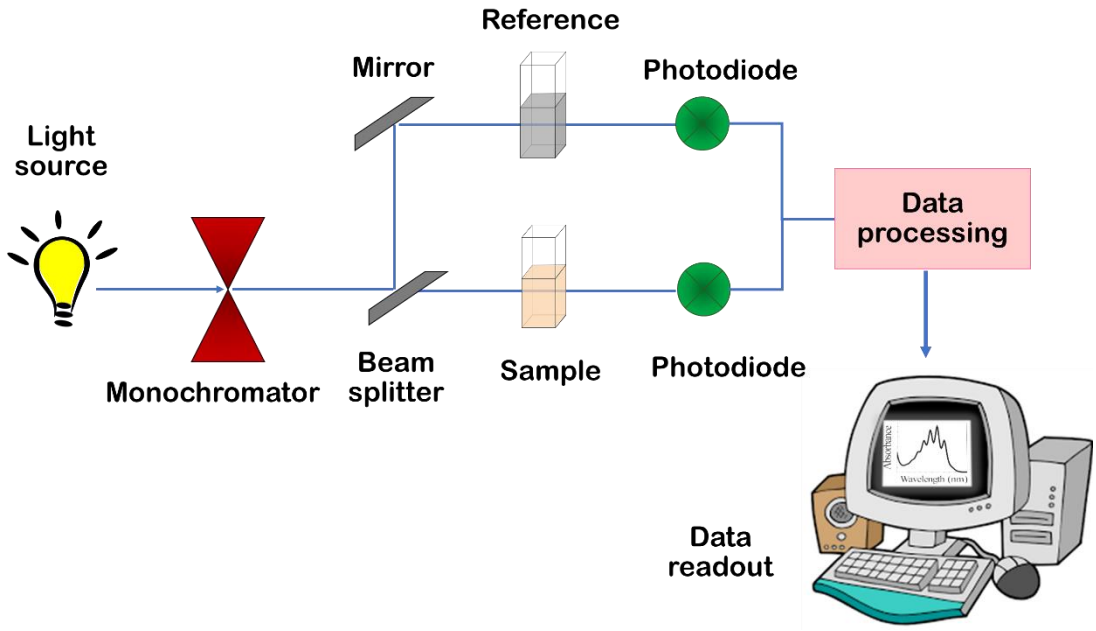

Figure 1.10 A schematic diagram of a double beam UV-Vis spectrophotometer.

The example of absorption spectrum is shown in Figure 1.11, which is a simple UV-Vis absorption spectrum of AuNPs. Absorbance (on the y axis) is a measure of the amount of light absorbed. The higher the value, the more of a particular wavelength is being absorbed. The wavelength that corresponds to the highest absorption is usually referred to as maximal wavelength (λ_{max}) that for example, λ_{max} is at 520 nm (Figure 1.11).

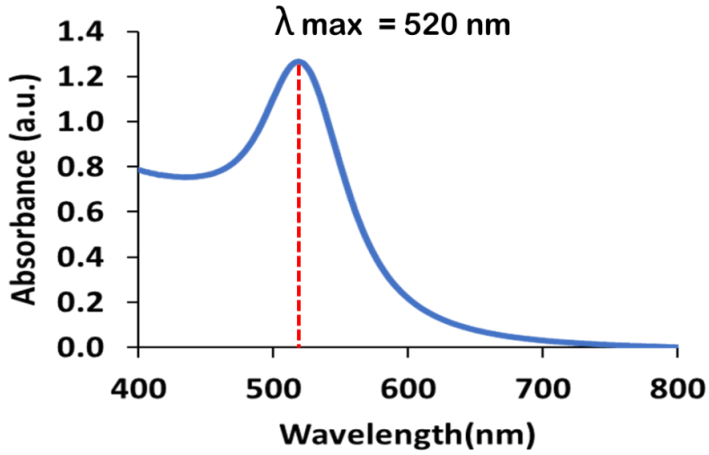

Figure 1.11 The absorption spectrum of AuNPs.

According to the Beer-Lambert's Law, the absorbance is proportional to the concentration of the sample. By this way, if we know the absorbance, we can determine the concentration of a sample. The Beer-Lambert's Law is expressed in Equation 1.1:

$$A = \varepsilon bC \qquad (1.1)$$

where A = the analyte absorbance

ε = the molar extinction, which is constant for a particular substance at a particular wavelength (L $mol^{-1}cm^{-1}$)

b = the cell pathlength, i.e. dimension of the cell or cuvette (cm). Commercial cell has 1 cm pathlength.

C = the concentration of analyte (mol L^{-1})

If the absorbance of a series of sample solutions of known concentrations are measured and plotted against their corresponding concentrations, the plot of absorbance versus concentration should be linear if the Beer-Lambert's Law is obeyed. This graph is known as a calibration graph. A calibration graph can be used to determine the concentration of analyte solution by measuring its absorbance.

1.2.3.2 Other techniques

Fumonisin B1 can be detected by various techniques as shown in Table 1.2.

Table 1.2 The detection techniques for determination of fumonisin B1 in different samples.

Detection techniques	Samples	Sample preparation	Linearity	LOD	References
High-performance liquid chromatography with diode array detector (HPLC-DAD)	Corn	Extracted with methanol and purified with solid-phase extraction (SPE) column	30-300 µg kg^{-1}	50 µg kg^{-1}	Krska et al., (1996)
High-performance liquid chromatography with fluorescence detector (HPLC-FLD)	Maize, gluten meal	Extracted with methanol: water and cleaned up with SPE column	3-8000 µg kg^{-1}	1 µg kg^{-1}	Coronel et al., (2016)
Liquid chromatography-Tandem mass spectrometry	Corn	Extracted with methanol: water and used ultrasonication	5-400 µg kg^{-1}	3.5 µg kg^{-1}	Li et al., (2012)
Enzyme-linked immunosorbent assay	Maize	Extracted with methanol: water	5-500 µg kg^{-1}	-	Sheng et al., (2012)
Colloidal gold immunoassay strip test	Corn	Extracted with methanol and conjugated with keyhole limpet hemoeyanin (KLH)	2.5-10 µg kg^{-1}	2.5 µg kg^{-1}	Ling et al., (2015)

1.2.4 Method validation

1.2.4.1 Linearity

A calibration curve is usually made in which the standard signal is plotted against the standard concentration under the same conditions (Garcia et al., 2011). The relationship between an instrument response and the known concentrations of an analyte or standards which is called as the calibration curve can be explained by regression line as seen in Figure 1.12. The linear equation is described in Equation 1.2. Linear regression is typically performed using a linear least-squares analysis. A perfect line would have the coefficient of determination (R^2) of 1, and most R^2 values for calibration curves are over 0.95. When the calibration curve is linear, the slope is a measure of sensitivity (Miller & Miller, 2015).

$$y = mx + c \qquad (1.2)$$

where y is the measured absorbance

x is the analyte concentration

m is the slope of calibration curve

c is the intercept on the y-axis

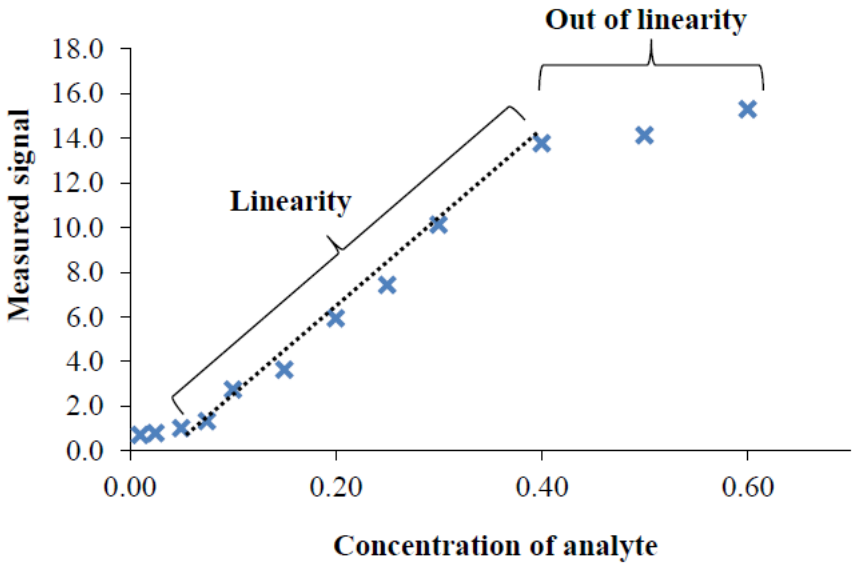

Figure 1. 12 The calibration plot with linear range and non- linear range response (Plaisen et al., 2018).

1.2.4.2 Limit of detection (LOD) and limit of quantification (LOQ)

Limit of detection (LOD) is the lowest concentration of analyte in sample which can be detected but not necessarily quantitated under stated experimental conditions. In general terms, LOD of an analyte can be describe as that analyte concentration gives an instrument signal (y) significantly different from the blank or background signal (Miller & Miller, 2015). LOD can be calculated as the concentration response corresponding to 3.3 times signal-to-noise (S/N = 3.3), as shown in Equation 1.3 (ICH,1996). Limit of quantification (LOQ) is the lowest concentration of an analyte which can be quantitatively determined with suitable precision and accuracy. LOQ is the amount that can be differentiated between samples and is usually defined as 10 times the noise (S/N = 10), as shown in Equation 1.4 (ICH, 1996).

$$LOD = 3.3 \frac{\sigma}{s} \quad (1.3)$$

$$LOQ = 10 \frac{\sigma}{s} \quad (1.4)$$

where σ is the standard deviation of the response which is estimated by the y-residual standard deviation of the regression line

s is the slope of the calibration curve

1.2.4.3 Matrix effect

In most samples, the matrix is the major component of the sample since the analyte has a relatively small concentration compared to matrices. Therefore, the chemical substances that make up the matrix may have an effect on the analysis, and most importantly, the measured response which we use to determine the concentration of the analyte.

The only way to deal with these problems is to modify the standards to make them more like the matrix (Cuadros-rodr et al., 2007). The methods include

- Standard addition curve: add series of known amount of analyte to aliquots of sample
- Matrix-matched standards curve: add series of the standards in the beginning step of sample preparation to make them as close as possible in composition or to obtain matrix-matched standards

The method of standard additions is a quantitative analysis method applied for spectrophotometry, electrochemical and chromatographic method to study matrix effect. The method is often used when the sample of interest has multiple components that result in matrix effects, where the additional components may either reduce or enhance the analyte absorbance signal (Thompson, 2009).

The matrix effect in term of standard addition curve can be perform by samples spiked with various concentration analyte. The matrix effect was evaluated by plotting the different concentration of analyte on x-axis and measurement signal on y-axis (Zhou et al., 2017). This method can indicate the effect of interference by comparing curve between the standard calibration and the standard addition curve. If slope of both are the same or similar which not significantly different based on statistical analysis, it can explain that the effect of interference in the sample does not affect the analysis (Miller & Miller, 2015) as shown in Figure 1.13.

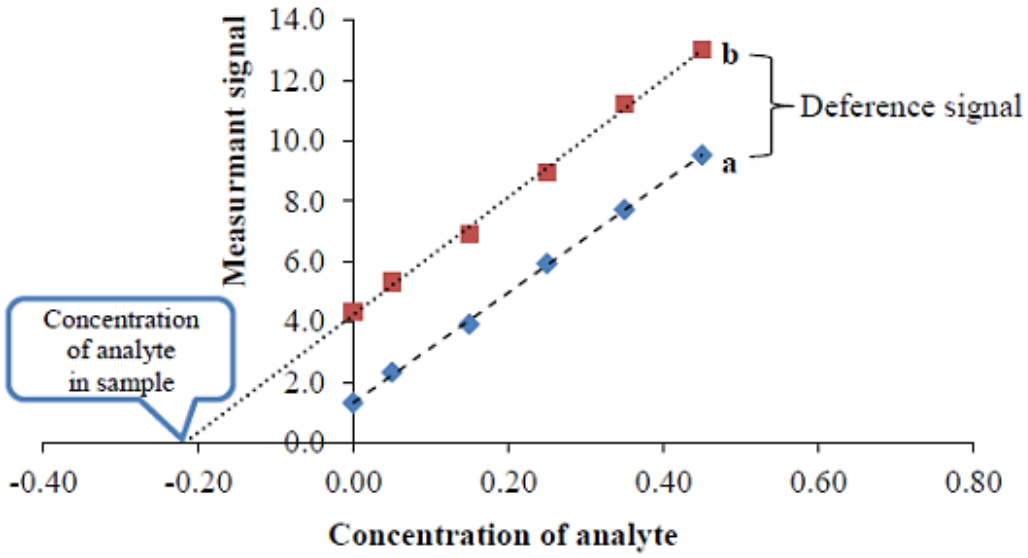

Figure 1.13 The plots of standard calibration curve and standard addition curve (Plaisen et al., 2018).

1.2.4.4 Accuracy

Accuracy is the closeness of agreement between a test result or a measurement result and the true value. The accuracy can be explained in a term of recovery which is studied by spiking known standard into the real sample. The percentage of recovery is calculated as described in Equation 1.5 (AOAC, 2012).

$$\% \text{ Recovery} = \frac{C_F - C_U}{C_A} \times 100 \qquad (1.5)$$

where C_F is the concentration of spiked sample with standard analyte

C_U is the concentration of unspiked sample

C_A is the concentration of standard added to sample

1.2.4.5 Precision

Precision describes data from an experiment that has been repeated several times. If the experiment yields a tightly grouped set of data points, then it has high precision. The greater the scatter of data points, the lower the precision. Precision can be evaluated by repeating measurements of the same sample in 3 to 6 replicates. The repeatability describes the precision of within-run replicate or intra-day and reproducibility describes the precision of between-run replicate or inter-day. Precision is usually reported as the standard deviation (SD) or relative standard deviation (RSD), as described in Equation 1.6 and 1.7, respectively (AOAC, 2012).

$$SD = \sqrt{\frac{\sum_{i=1}^{n} (X_i - \bar{X})^2}{n-1}} \qquad (1.6)$$

$$\% \text{ RSD} = \frac{SD}{\bar{X}} \times 100 \qquad (1.7)$$

where n is the total number of measurements

X is the mean of measurement

X_i is the number of measurements

1.3 Objectives

1. To develop the colorimetric method based on aggregation of Cyst-AuNPs for fumonisin B1 detection.

2. To apply the developed sensor for fumonisin B1 determination in corn samples.

1.4 Benefit

Robust colorimetric detection of fumonisin B1 based on hydrolyzed product induced aggregation of cysteamine functionalized gold nanoparticles is simple, highly sensitive and selective. The method can be easily observed by the naked eyes or measured by UV-Vis spectrophotometry. Morevore, it has been proved to be applied in real corn samples.

CHAPTER 2
EXPERIMENTAL

2.1 Overall scope

The colorimetric method for determination of fumonisin B1 (FB1) based on aggregation of modified gold nanoparticles (Cyst-AuNPs) was developed and applied in corn samples. The overall scope of work was studied according to the chart shown in Figure 2.1.

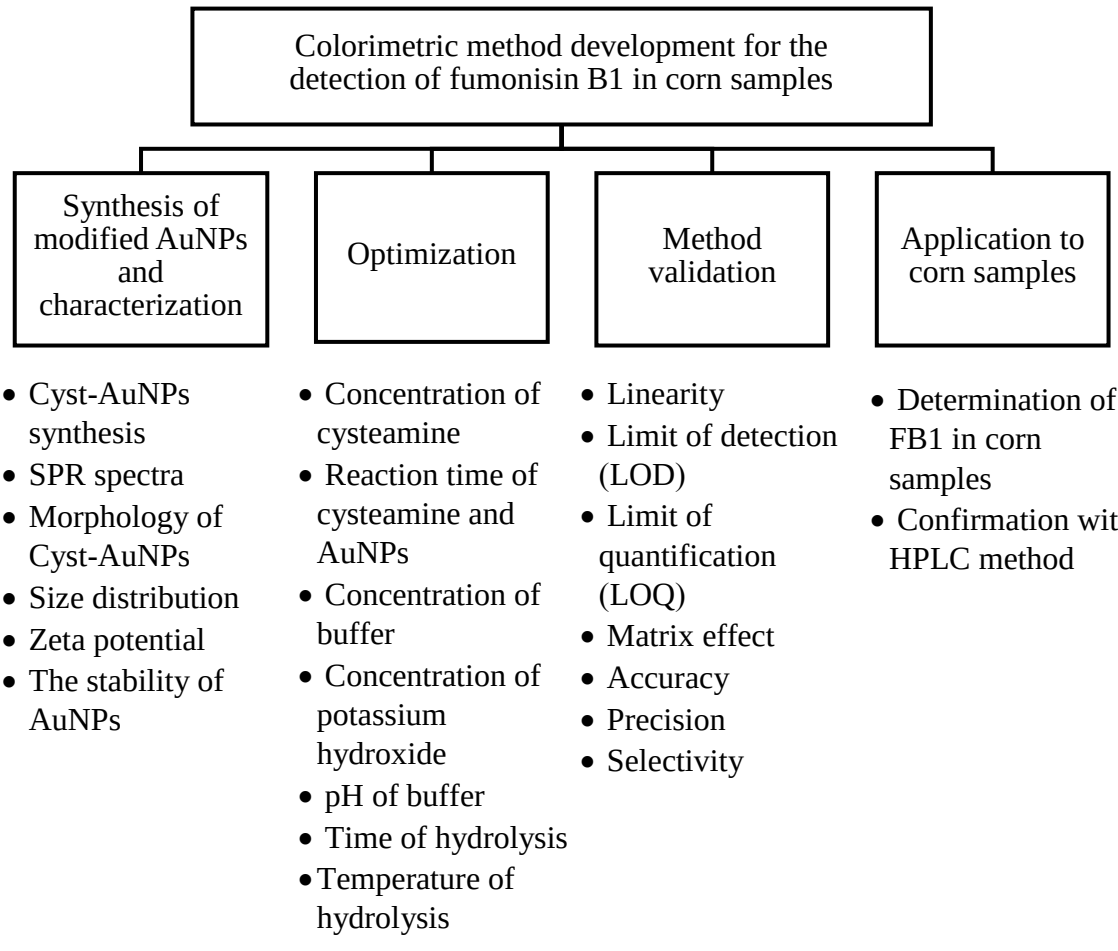

Figure 2.1 The scope of method for fumonisin B1 detection in corn sample using colorimetric method based on the aggregation of Cyst-AuNPs.

2.2 Chemicals and reagents

All chemicals and reagents were purchased from several companies, and were of analytical and HPLC grade, as shown in Table 2.1 and 2.2, respectively. In this work, the solutions were prepared using 18 MΩ cm ultrapure water obtained from ELGA Maxima (England) for all experiments.

Table 2.1 Chemicals and reagents (analytical grade) used for fumonisin B1 analysis.

Chemicals and reagents	Brand	Country
Acetic acid	RCI Labscan	Thailand
Acetonitrile	RCI Labscan	Thailand
Boric acid	RCI Labscan	Thailand
Cysteamine	Sigma-Aldrich	USA
Hydrogen tetrachloroaurate	Sigma-Aldrich	USA
Nitric acid	RCI Labscan	Thailand
Phophoric acid	RCI Labscan	Thailand
Potassium hydroxide	RCI Labscan	Thailand
Sodium hydroxide	RCI Labscan	Thailand
Trisodium citrate	Ajax Finechem	Australia

Table 2.2 Chemicals and reagents (HPLC grade) used for fumonisin B1 analysis.

Chemicals and reagents	Brand	Country
Acetonitrile	RCI Labscan	Thailand
Alflatoxin	Biopure	USA
Citrinin	Sigma-Aldrich	USA
Fumonisin B1	Calbiochem	USA
Methanol	RCI Labscan	Thailand
Patulin	Sigma-Aldrich	USA
Zearalenone	Sigma-Aldrich	USA

2.3 Laboratory glassware

2.3.1 Glassware

1) Amber bottle 100 mL
2) Beaker 25 mL, 50 mL, 150 mL, 250 mL and 1000 mL
3) Cylinder 10 mL, 25 mL and 100 mL
4) Dropper
5) Glass bottle 250 mL
6) Glass rod
7) Vial with screw cap 2 mL
8) Volumetric flask 5 mL, 10 mL, 25 mL, 100 mL and 250 mL
9) Watch glass

2.3.2 Cleaning of glassware

All glassware was cleaned with detergent solution and washed with tap water. Then it was rinsed with distilled water and immersed in 10% (v/v) nitric acid for about 12 hours and washed with distilled water. Finally, it was dried in the oven at 150˚C for 2 hours (Caution: Do not dry volumetric flask and cylinder in the oven).

Glassware used for storage and synthesis of gold nanoparticles solution, such as beakers, volumetric flask, cylinder, amber bottle and magnetic bar must be specially cleaned to prevent the aggregation of AuNPs. When general cleaning of glassware is completed, then a freshly prepared aqua regia solution 3:1 (v/v) of HCl:HNO_3 is further used for cleaning, then washed with ultrapure water for several times and dried in the oven at 150˚C for 2 hours.

2.4 Apparatus and materials

All apparatus and materials used for fumonisin B1 analysis are listed in Table 2.3.

Table 2.3 The apparatus and materials used for fumonisin B1 analysis

Apparatus and materials	Brand	Country
Analytical balance 0.0001 g	Mettler Toledo	Switzerland
Bench top pH meter	BANTE Instruments	China
Centrifuge machine	Hermie Labortechnik GmbH	Germany
Centrifuge tube 50 mL	Biologix	China
Disposable polystyrene cuvette	VWR We Enable Science	Germany
Dri-Block Heater	Techne	UK
Freezer	UMA'C Scientific	China
HLB extraction cartridge	OASIS, Waters Corporation	USA
Hot air oven	Memmert	Germany
Hot plate and stirrer	IKA, C-MAGHS7	Germany
iPhone 7 plus (digital camera)	Apple	USA
Magnetic bar	-	-
Micro pipette 100-1000 µL	Thermo Scientific	USA
Micro pipette 20-200 µL	Thermo Scientific	USA
Micro pipette 5-50 µL	CAPP Bravo	Denmark
Microtube	Axygen	USA
Nylon membrane filters 0.22 µm	Agela Technologies	USA
Refrigerator	TOSHIBA	Japan
SPE Manifold	Aglilent Technologies	USA
Syringe	TERUMO	Phippines
Vacuum pump	GAST	USA

2.5 Instruments

2.5.1 UV-Visible spectrophotometer

Ultraviolet-visible (UV-Vis) absorption spectra were recorded with A UV-2600 spectrophotometer (Shimadzu, Japan) in the wavelength range of 400-800 nm using a 1.5 mL disposable polystyrene cuvette.

2.5.2 Fourier transform infrared spectroscopy (FTIR)

Fourier transform infrared spectroscopy (Vertex70, Bruker, Germany) was used for recording the functional group of modified AuNPs (Cyst-AuNPs).

2.5.3 Transmission electron microscopy (TEM)

A transmission electron microscope (TEM) was performed on a JEM-2010, JEOL (Japan) instrument at a 200 kV acceleration voltage. It was used to investigate the morphology including size, shape, dispersion state and aggregation state of AuNPs and modified AuNPs.

2.5.4 Zeta potential analyzer

A zeta potential was performed on a ZetaPALS, Brookhaven (USA) for zeta potential and size distribution of AuNPs and modified AuNPs solution.

2.6 Preparation of solution

2.6.1 Preparation of standard solution of fumonisin B1

1. A stock solution containing 250 mg L^{-1} of fumonisin B1 was prepared by dissolving 1 mg of fumonisin B1 with 4 mL methanol. An aliquot of standard solution was transferred to 1.0 mL amber vials for single use. The standard solution was stored at -20˚C in freezer when not in use.

2. A working solution containing 10 mg L^{-1} of fumonisin B1 was prepared by transferring 200 µL of 250 mg L^{-1} of fumonisin B1 to 5 mL of (20:80 v/v) ACN:H_2O (Tharkur et al., 1996). The mixture of ACN:H_2O was used for dissolving solution because it was found that methanol causes AuNPs unstable, resulting in variation of colorimetric detection.

2.6.2 Preparation of 0.015% w/v gold(III) chloride solution

150 mL of 0.015% w/v gold (III) chloride trihydrate was prepared by dissolving 0.0225 g of gold(III) chloride trihydrate in ultrapure water and the volume was adjusted to 150 mL in volumetric flask, then kept in refrigerator before further synthesis.

2.6.3 Preparation of 1% (w/v) trisodium citrate solution

10 mL of 1% (w/v) trisodium citrate was freshly prepared by dissolving in ultrapure water and adjusted volume to 10 mL in volumetric flask.

2.6.4 Preparation of 0.01 µM cysteamine

A 250 mL of 0.01 M cysteamine was prepared by dissolving 0.1929 g of cysteamine in ultrapure water and volume was adjusted to 250 mL in volumetric flask.

A 250 mL of 0.1 mM cysteamine was diluted from 0.01 M cysteamine. It was prepared by transferring 2.5 mL of 0.01 M cysteamine to volumetric flask and volume was adjusted to 250 mL.

A 250 mL of 0.01 µM cysteamine (working solution) was prepared by diluting 0.1 mM cysteamine. It was transferred 25 µL of 0.1 mM cysteamine to volumetric flask and was made up to 250 mL.

2.6.5 Preparation of 10 mM Britton-Robinson buffer

Britton-Robinson buffer in the pH range of 3.0-12.0 was prepared by mixing 0.01 M of phosphoric acid, 0.01 M of acetic acid and 0.01 M of boric acid. The buffer was adjusted to different pH by adding 0.1 M sodium hydroxide**.**

2.7 The synthesis and modification of gold nanoparticles

2.7.1 The synthesis of gold nanoparticles solution

The synthesis of gold nanoparticles solution is shown in Figure 2.2. A 150 mL aqueous solution of $HAuCl_4$ (0.015%, w/v) was added to a 250 mL beaker and brought to a vigorous boil with stirring, and then 5.25 mL of sodium citrate (1% w/v) was rapidly injected into the solution to reduce the Au^{3+} to Au^0. The citrate anions also helped to stabilize the AuNPs. The color of the solution changes from yellow to purple, and finally changed to ruby red in few minutes. After that, the solution was boiled continuously for 15 min to ensure the reaction was completed. The AuNPs solution was cooled to room temperature and stored in an amber glass bottles at 4˚C in refrigerator for further use.

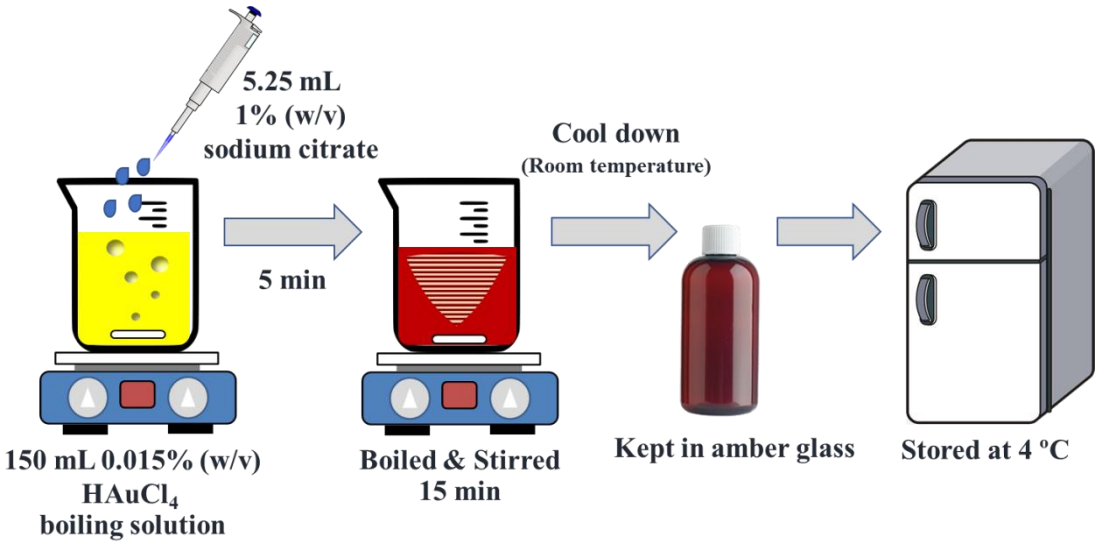

Figure 2.2 The synthesis of gold nanoparticles.

2.7.2 The modification of gold nanoparticles surface

Preparation of cysteamine capped gold nanoparticles (Cyst-AuNPs) was achieved by the following step. A 60 mL of AuNPs solution was diluted with 30 mL of ultrapure water (0.5-fold) and mixed with 10 mL of 0.01 µM cysteamine in the ratio of AuNPs: Cyst (9:1) by stirring for 5 min as shown in Figure 2.3.

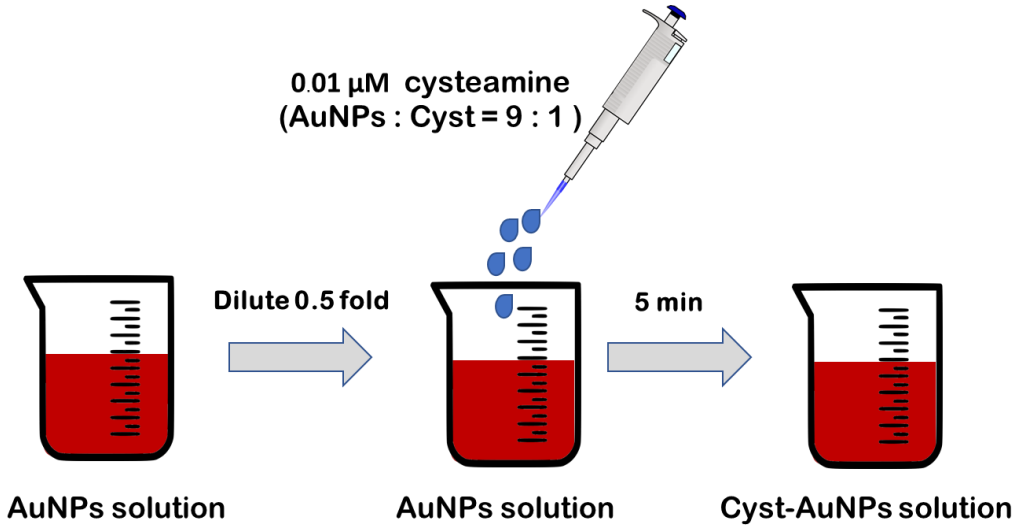

Figure 2.3 The modification of gold nanoparticles surface.

2.8 Characterization of modified gold nanoparticles (Cyst-AuNPs)

2.8.1 The surface plasmon resonance (SPR)

The surface plasmon resonance (SPR) spectra were measured in the range of 400-800 nm by UV-2600 spectrophotometer (Shimadzu, Japan). The mixture solution was contained in a 1.5 mL disposable polystyrene semi cuvette. It was measured by spectrophotometer with following conditions. Condition of spectrophotometer

- Scan rate: Fast mode
- Slit width: 1.0 nm
- Sampling interval: 1.0 nm
- Wavelength range: 400-800 nm
- Reference sample: Ultrapure water

2.8.2 Fourier transform infrared spectroscopy (FTIR)

The cysteamine functionalized AuNPs was confirmed by FTIR spectroscopy (Vertex70, Bruker, Germany). For preparation sample, cysteamine powder was stored in a desiccator before mixing with KBr prior to measure. Cysteamine-AuNPs solution was freeze dried to powder. Then sample powder was well mixed with KBr to measure by FTIR instrument.

2.8.3 Transmission electron microscopy (TEM)

The morphology of modified gold nanoparticles (size and shape of cyst-AuNPs) was measured by transmission electron microscopy (TEM, JEM-2010, JEOL, Japan) at a 200-kV acceleration voltage.

The preparation of sample solution

1. Dispersed Cyst-AuNPs; the AuNPs solution was capped with cysteamine in the ratio of AuNPs:Cyst (9:1). It was used to study size, shape and dispersion state of Cyst-AuNPs.
2. Aggregated Cyst-AuNPs; the mixture solution of Cyst-AuNPs, 10 mM Briton-Robinson buffer and 10 mg L^{-1} hydrolyzed fumonisin B1 (HFB1) were prepared to study aggregation state of Cyst-AuNPs.

The sample solution was prepared by two times dilution with ultrapure water. 5 μL of diluted sample was deposited on the carbon coated copper grid and then incubated at room temperature for 2 days.

The size of particle was measured with TEM and calculated by software ImageJ version 1.51 k.

2.8.4 Zeta-potential analysis

The study of charge value and stability on the surface of AuNPs was determined by zeta potential analyzer (ZetaPALS, Brookhaven,USA) with the software of ZetaPaLS Potential Analyzer version 3.54.

The preparation of sample solution

1) AuNPs; 1 mL of AuNPs
2) Cyst-AuNPs; the mixture solution of Cyst-AuNPs and 10 mM Briton-Robinson buffer
3) Aggregated-AuNPs; the mixture solution of Cyst-AuNPs, 10 mM Briton-Robinson buffer and 10 mg L^{-1} HFB1

2.8.5 Size distribution analysis

The size distribution of Cyst-AuNPs and aggregated AuNPs were performed on zeta potential analyzer (ZetaPALS, Brookhaven,USA) with the software of ZetaPaLS Particle Sizing version 4.03. The sample obtained from section 2.8.3 was diluted two times with ultrapure water before measurement.

2.9 Optimization of parameters affecting the fumonisin B1 sensor

To achieve the optimum conditions for fumonisin B1 detection, detailed optimization of parameters were carried out i.e., concentration of cysteamine, reaction time of cysteamine and AuNPs, pH of buffer, concentration of buffer, concentration of alkaline media, time of hydrolysis and temperature of hydrolysis. Each parameter was studied while other parameters were kept constant. All experiments were repeated three times with a report of mean ± standard deviation (SD). Statistical analyses were evaluated using the Microsoft Excel software, version 2016.

2.9.1 Optimization of cysteamine functionalized on AuNPs surface

2.9.1.1 Effect of cysteamine concentration

Cysteamine was used as the capping agent. Therefore, an appropriate concentration of cysteamine in the system was optimized. The effect of concentration of cysteamine was studied in the range of 0.001-10.0 μM. It was performed by adding 900 μL of AuNPs solution and 100 μL of different concentrations of cysteamine to a 1.5 mL microtube, respectively. The mixture was shaken by hand before measurement by UV-Vis spectrophotometry and the photograph was taken by digital camera.

2.9.1.2 Reaction time of cysteamine binding to AuNPs

The effect of reaction time was studied in the range of 5-30 minutes for cysteamine capped on AuNPs surface. It was performed by adding 0.01 μM cysteamine into AuNPs solution (AuNPs:cysteamine, 9:1). The mixture was shaken by hand before measurement by UV-Vis spectrophotometry and the photograph was taken by digital camera.

2.9.2 Optimization of alkaline hydrolysis

2.9.2.1 Effect of alkaline hydrolysis of fumonisin B1

Potassium hydroxide (KOH) was used for the hydrolysis and the concentration was investigated in the range of 0.5-1.3 M. Hydrolysis of fumonisin B1 was performed by adding 1.2 mL of sample solution and 0.8 mL of different concentrations of KOH in a 4 mL closed vial. The mixture was heated at 70˚C for 1 h. To neutralize solution, the hydrolyzed solution (called as HFB1) was added with 500 μL of 1 M nitric acid. The hydrolyzed solution was onefold diluted with ultrapure water before reacting with Cyst-AuNPs.

2.9.2.2 Time of hydrolysis

The influence of hydrolysis time was studied ranging from 10-100 min upon the interaction between 1.2 mL of 10 mg L^{-1} FB1 and 0.8 mL of 1.0 M KOH. The mixture was heated at 70˚C for different hydrolysis times. Each time, the solution was added with 500 µL of 1 M nitric acid to neutralize solution. Finally, the hydrolyzed solution was reacted with Cyst-AuNPs before measurement by UV-Vis spectrophotometry.

2.9.2.3 Temperature of hydrolysis

The influence of hydrolysis temperature from 30-90˚C was investigated. It was performed in the same way as mentioned in section 2.9.6. Then, the mixture was heated at different temperatures for 1 h before reacting with Cyst-AuNPs.

2.9.3 Optimization of colorimetric detection based on Cyst-AuNPs

2.9.3.1 The effect of pH of Britton-Robinson buffer

The effect of pH was optimized from 3.0 to 12.0 using 10 mM of Britton-Robinson buffer. It was performed by adding 600 µL of Cyst-AuNPs, 200 µL of 10 mM Britton-Robinson buffer (different pH) and 50 µL of 10 mg L^{-1} of HFB1 in a microtube. After mixed and shaken by hand, the absorbance was measured by UV-Vis spectrophotometry.

2.9.3.2 The concentration of Britton-Robinson buffer

The effect of concentration of Britton-Robinson buffer (pH 9) was studied in the range from 1-50 mM. The reaction was initiated by mixing 600 µL of cyst-AuNPs, 200 µL of different concentrations of Britton-Robinson buffer (pH 9) and 50 µL of 10 mg L^{-1} of HFB1 in a microtube. It was shaken and measured by UV-Vis spectrophotometry.

2.10 Hydrolysis of fumonisin B1

The hydrolyzed fumonisin B1 (HFB1) was prepared from 10 mg L^{-1} of stock FB1 solution using base hydrolysis and with controlled time and temperature of the reaction. Complete hydrolysis was achieved by mixing 1.2 mL of the 10 mg L^{-1} of stock FB1 with 0.8 mL of 1 M KOH and heating the mixtures in a closed vial at 70˚C for 1 h by using a dri-block heater as shown in Figure 2.4. The hydrolysis was stopped by neutralized the solutions to pH 7.0 with an addition of 1 M HNO_3.

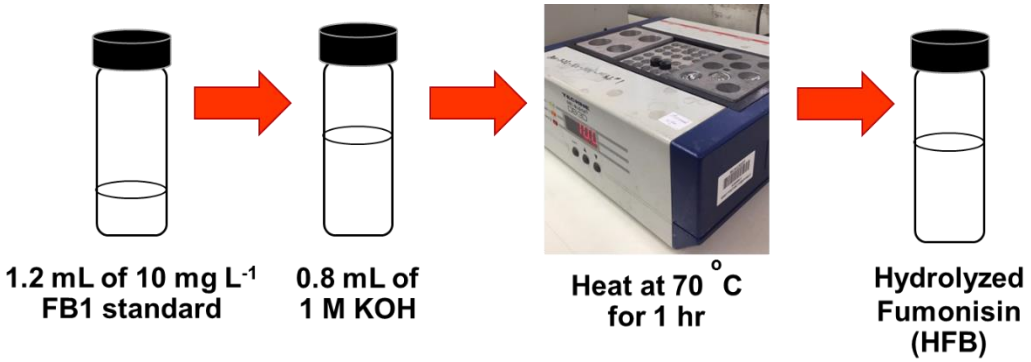

Figure 2.4 The hydrolysis procedure of fumonisin B1.

2.11 Overall colorimetric determination of fumonisin B1

For the detection of fumonisin B1 as shown in Figure 2.5, 200 µL of 10 mM Britton-Robinson buffer at pH 9 was added to 600 µL Cyst-AuNPs. The solution was shaken and 50 µL of different concentration of neutral hydrolyzed fumonisin B1 was added. The mixture solution was shaken. The color of solution gradually varied from wine red to blue gray with the increasing concentration of fumonisin B1. After interaction, the photographs of resulting solution were taken and the UV-Vis spectra of the mixtures from 400-800 nm were recorded. The real samples were investigated with the same procedure.

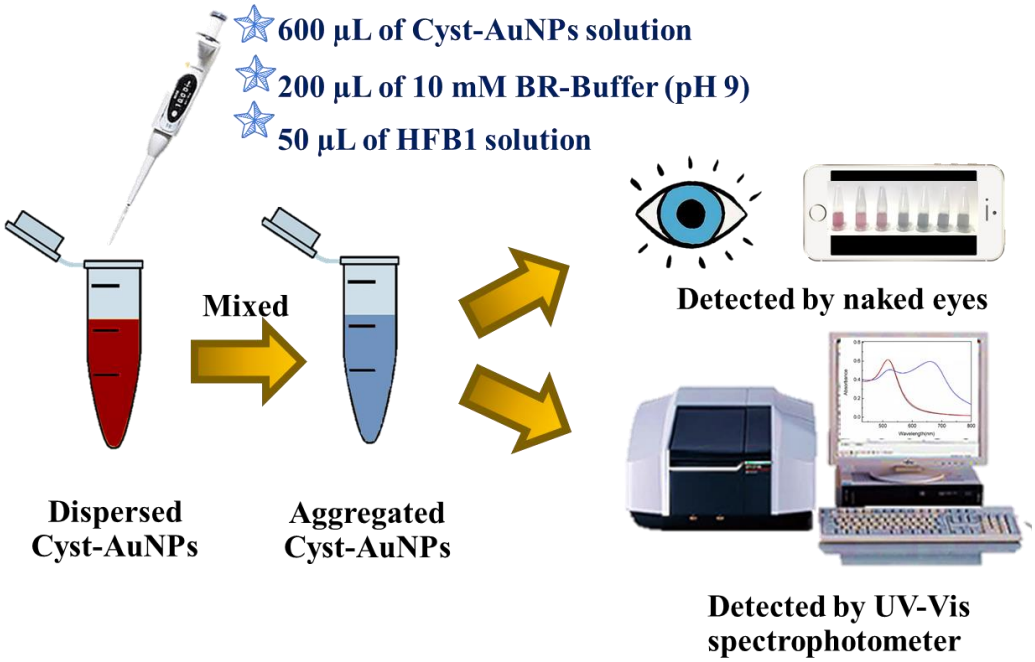

Figure 2.5 The colorimetric detection procedure of fumonisin B1.

2.12 Method validation for fumonisin B1 determination

2.12.1 Linearity

The final concentration of fumonisin B1 at 2.0, 3.0, 4.0, 6.0, 8.0 and 10.0 µg L^{-1} were studied for a linearity of developed method. In the first step, each of the concentrations of fumonisin B1 was hydrolyzed as method mentioned in section 2.10. After that, the hydrolyzed solution was performed as colorimetric method in section 2.11. The linearity was plotted between the absorbance ratio (A_{645}/A_{520}) and concentration of fumonisin B1.

2.12.2 Limit of detection (LOD) and limit of quantification (LOQ)

Limit of detection (LOD) is the lowest concentration of fumonisin B1 in corn sample, which can be detected but not necessarily quantitated under stated experimental conditions (ICH, 1996).

Limit of quantification (LOQ) is the lowest concentration of fumonisin B1, which can be quantitatively determined with suitable precision and accuracy (ICH, 1996).

LOD and LOQ were calculated by the equation 3.3 σ/*s* and 10 σ/*s*, respectively, where σ is the standard deviation of the response which is estimated by the y-residual standard deviation of the regression line and s is the slope of the calibration curve (ICH,1996).

2.12.3 Matrix effect

2.12.3.1 Sample preparation

Corn sample was crushed through a blender and stored in ziplock plastic bags at 20˚C. The sample was extracted according to a previous report (Young et al., 2017). Briefly, 2.0 g was weighted into a 50 mL centrifuge tube. Subsequently, 10 mL ultrapure water and 10 mL of formic acid/acetonitrile (1:9, v/v) were added. The tube was shaken vigorously by hand for 1 min. Then 1.0 g trisodium citrate dihydrate, 0.5 g disodium hydrogencitrate sesquilhydrate, 1.0 g sodium chloride and 4.0 g magnesium sulfate were added and extracted by ultrasonication for 30 min, followed by centrifugation at 6000 rpm for 20 min. A portion of the supernatant was taken for clean-up by solid phase extraction.

The clean-up procedure was performed as follows: an Oasis PRiME HLB Cartridge (3 mL, 150 mg) was mounted on a pre-cleaned vacuum manifold. The supernatant was passed through the Oasis PRiME Cartridge and collected in a 20 mL glass vial. A 4 mL of sample extract was evaporated under a gentle nitrogen stream, and re-dissolved with 2 mL of acetonitrile/ultrapure water (20:80, v/v). The solution was ultrasonicated for 20 min and then 1.2 mL of solution was taken to hydrolyze by alkaline hydrolysis. Finally, the hydrolyzed sample solution was then one-fold diluted with ultrapure water before color reaction.

2.12.3.2 The standard addition method

The effect of matrix on the developed method was studied by using a standard addition curve spiked with fumonisin B1 in the range of 2.0-10.0 µg L^{-1} into corn sample extracts obtained from section 2.12.3.1. After that, corn sample extracts were hydrolyzed before colorimetric detection. The slope of the standard addition curve was compared with a standard calibration curve at same concentration range.

2.12.4 Accuracy

The accuracy of developed method was investigated by a recovery method (AOAC, 2012). Three concentrations of fumonisin B1 (16.55, 33.01 and 49.37 mg kg^{-l}) were spiked into composite corn samples to obtain final concentrations of 2.0, 4.0 and 6.0 µg kg^{-1}, respectively. All spiked and unspiked samples were performed as mention in section 2.12.3.1.

2.12.5 Precision

The precisions of developed method were performed in terms of intra-day and inter-day and reported as relative standard deviation (RSD). Three concentrations of FB1 (2.0, 6.0 and 10.0 µg L^{-1}) were studied. The intra-day precision was measured in 5 replicates on the same day. The intra-day precision was measured in 3 replicates for 5 different days. Each measurement was prepared as following method in section 2.10 and 2.11.

2.13 Selectivity

The influence of other mycotoxins which can be found in corn samples were investigated. The other mycotoxins including aflatoxin, zearalenone, citrinin and patulin were studied with 3 replicates under the optimum conditions. The absorbance ratio (A_{645}/A_{520}) and color detection was compared between 6.0 µg L^{-1} of fumonisin B1, 12.0 µg L^{-1} of each mycotoxin (aflatoxin, zearalenone, citrinin and patulin), and the

mixture of 6.0 μg L^{-1} of fumonisin B1 and 12.0 μg L^{-1} of aflatoxin, zearalenone, citrinin and patulin.

2.14 Application of the developed method to corn samples

2.14.1 Sample collection

Corn kernels (four samples) were collected randomly from the market in Songkhla province, Thailand. It was crushed through a blender and stored in ziplock plastic bags at -20˚C. The ground corns supplied by the National Corn and Sorghum Research Center (Bangkok, Thailand) were also investigated.

2.14.2 Determination of fumonisin B1 in corn samples

2.14.2.1 Overall sample preparation

The sample preparation was performed according to a previous report (Young et al., 2017). Two grams of sample was weighted into a 50 mL centrifuge tube. Next, 10 mL ultrapure water and 10 mL of formic acid/acetonitrile (1:9) were added. The tube was shaken vigorously by hand for 1 min. Then 1.0 g trisodium citrate dihydrate, 0.5 g disodium hydrogencitrate sesquilhydrate, 1.0 g sodium chloride and 4.0 g magnesium sulfate were added and extracted by ultrasonication for 30 min, followed by centrifugation at 6000 rpm for 20 min. A portion of the supernatant was taken for clean-up by solid phase extraction.

The clean-up procedure was performed as follows: an Oasis PRiME HLB Cartridge (3 mL, 150 mg) was mounted on a pre-cleaned vacuum manifold. The supernatant was passed through the Oasis PRiME Cartridge and collected in a 20 mL glass vial. 4 mL of sample extract was evaporated under a gentle nitrogen stream, and re-dissolved with 2 mL of acetonitrile/ultrapure water (20:80, v/v). The solution was ultrasonicated for 20 min and then 1.2 mL of solution was taken to hydrolyze by alkaline hydrolysis. Finally, the hydrolyzed sample solution was then one-fold diluted with ultrapure water before color reaction.

2.14.2.2 Colorimetric assay of fumonisin B1 in corn samples

For the detection of fumonisin B1 in corn samples, after the real samples were extracted and cleaned-up. 200 µL of 10 mM Britton-Robinson buffer at pH 9 was added into 600 µL Cyst-AuNPs. The solution was shaken and added with 50 µL of hydrolyzed sample solution. The mixture solution was shaken. The color of solution gradually varied from wine red to blue grey with the increasing concentration of fumonisin B1. After reacting, the photographs of resulting solution were taken and the UV-Vis spectra of the mixtures from 400-800 nm were recorded.

2.15 Confirmation of fumonisin B1 determination with high-performance liquid chromatography with fluorescence detector (HPLC-FLD)

2.15.1 Sample preparation for HPLC analysis

5.0 g of corn samples was added with 100 mL of methanol:water (3:1, v/v). After that, the mixture was shaken for 15 min and was filtered by suction filtration (FAMIC, 2008).

The clean-up method is as follows: the Bond Elut LRC SAX cartridge (1 g, 6 mL) was washed with 8 mL methanol and 8 mL methanol:water (3:1, v/v). 10 mL of the sample solution was loaded on the cartridge. Then 8 mL of methanol:water (3:1) and 8 mL of methanol was added sequentially to the cartridge and eluted similarly. 14 mL of methanol:acetic acid (99:1, v/v) was add to the cartridge to elute fumonisin B1 and kept in a 20 mL vial. The eluate was concentrated and dried under nitrogen gas. The residue was dissolved by the addition of 1 mL of acetonitrile:water (1:1, v/v) and the solution was filtered through a 0.22 µm nylon membrane. Before injection onto HPLC, the solution was derivatized with 200 µL of o-phthaldialdehyde for 2 min at room temperature.

2.15.2 HPLC-FLD condition

The condition of high-performance liquid chromatography with fluorescence detector (1200 Agilent, USA) as follows (FAMIC, 2008);

Column type: C18 column (5 μm, 250×4.6 nm)

Mobile phase: MeOH:NaH_2PO_4 (75:25, v/v)

Flow rate: 1 mL min^{-1}

Column temperature: 30˚C

Excitation wavelength: 335 nm

Emission wavelength: 440 nm

2.16 Statistics

All the statistical analyses were performed using one-way ANOVA at 95% confidence level in Microsoft Office Excel 2016.

CHAPTER 3

RESULTS AND DISCUSSION

A simple and selective method based on the aggregation of cysteamine capped gold nanoparticles (Cyst- AuNPs) was established for colorimetric detection of fumonisin B1. The aggregation of Cyst- AuNPs was reflected by the change in color (wine-red to blue-grey) and absorption spectra (520 nm to 645 nm) that can be observed by the naked eyes and measured by a UV-Vis spectrophotometer.

3.1 Synthesis of gold nanoparticles (AuNPs)

Gold nanoparticles (AuNPs) were produced in a liquid phase through chemical method by the reduction of chloroauric acid ($HAuCl_4$). After dissolving $HAuCl_4$, the solution was stirred while a reducing agent (trisodium citrate dihydrate) was rapidly added. This causes Au^{3+} ions to be reduced to neutral gold atoms (Au^0), as shown in equation 3.1. The citrate anions also stabilize the colloidal AuNPs.

$$6(AuCl_4)^- + C_6H_8O_7 + 5H_2O \text{ ----------> } 4CO_2 + 24Cl^- + 6Au^0 + 18H^+ \qquad (3.1)$$

The synthesis of AuNPs was performed as described in section 2.7.1. As shown in Figure 3.1, the solution color changed from yellow (Figure 3.1a) to colorless (Figure 3.1b), to dark purple (Figure 3.1c) and finally to wine red (Figure 3.1d) within around 5 min.

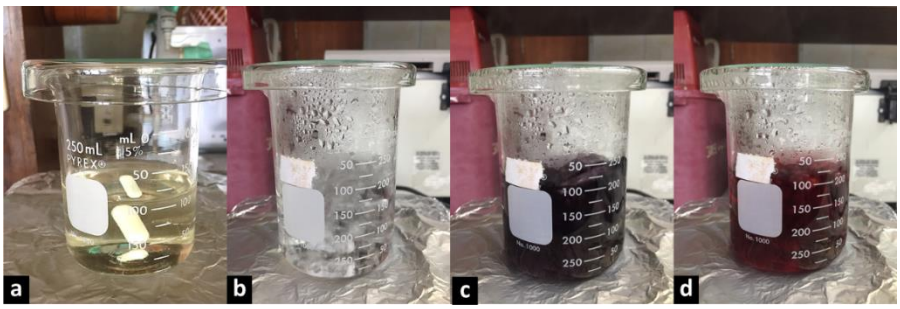

Figure 3.1 The color changes of aqueous solution in AuNPs preparation.

The wine-red solution of AuNPs demonstrated the surface plasmon resonance (SPR) phenomenon with absorption measured by UV-Vis spectrophotometry, with the AuNPs (diluted 0.5-fold) having the maximum wavelength of 520 nm when the scanning was performed within 400 to 800 nm as shown in Figure 3.2.

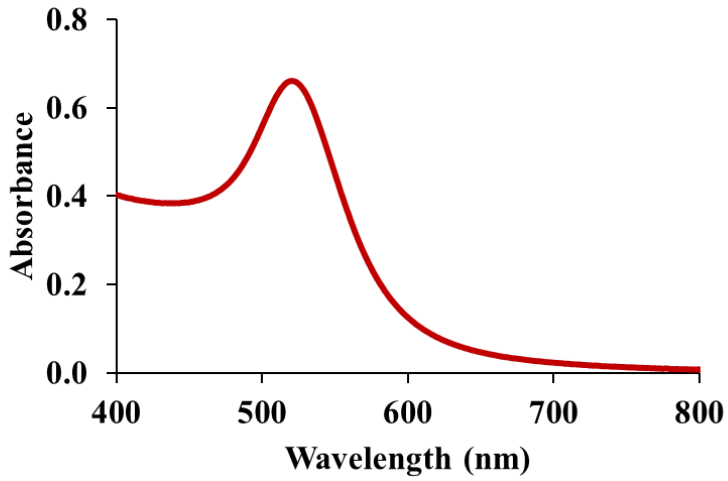

Figure 3.2 UV-Vis absorption spectrum of the synthesized AuNPs (diluted 0.5-fold).

The concentration of AuNPs was calculated from Beer's Law with the extinction coefficient for ~13 nm AuNPs of about 2.70×10^8 M^{-1} cm^{-1} at ~520 nm (Chen et al., 2013). The concentration of the prepared AuNPs solution is about 4.7 nM. Furthermore, the size of particle was measured from TEM image of AuNPs as shown

in Figure 3.3. It was randomly measured, by taking the average diameters of 100 particles with ImageJ software. In Figure 3.3, the size distribution of AuNPs was found to be 13.3 ± 1.0 nm. Therefore, the synthesis of AuNPs has been confirmed to be successful. The size of dispersed AuNPs agreed well with previous reports (Sliem et al., 2007).

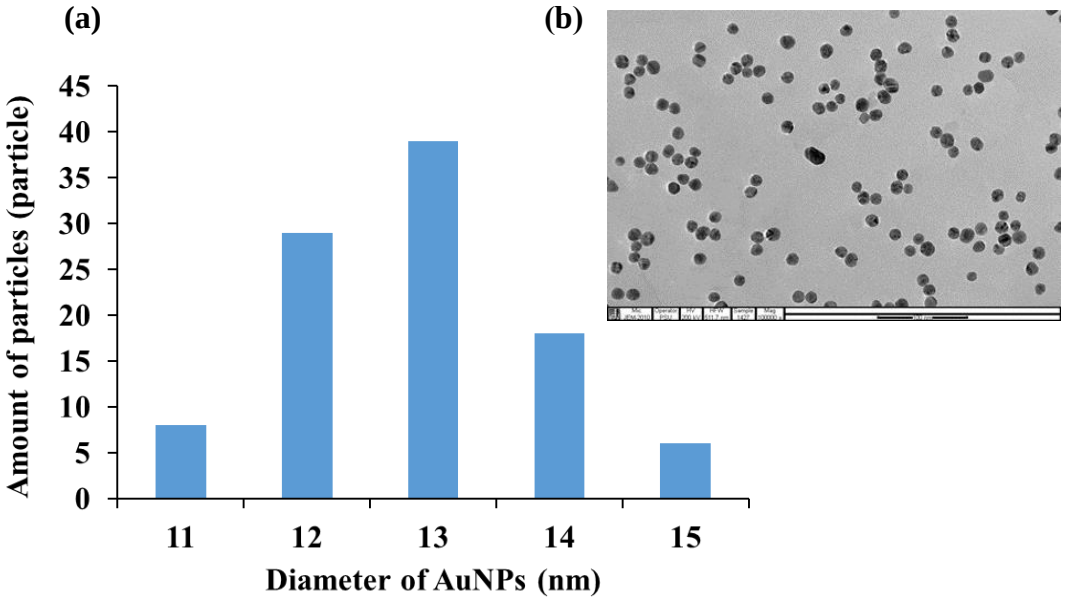

Figure 3.3 (a) The histograms of 100 particles size. (b) The TEM image of dispersed AuNPs.

3.2 Proposed sensing mechanism

Gold nanoparticles were first prepared by using sodium citrate reduction method. The citrate ions can act as a reductant and a stabilizer (Liu et al., 2016). The AuNPs were wine-red in color due to the strong electrostatic repulsion of negatively charge citrate ions on AuNPs surface (Zhou et al., 2014). As shown in figure 3.2, the AuNPs showed an absorption peak at 520 nm, which was ascribed to the surface plasmon resonance phenomenon. In this work, citrate-stabilized AuNPs was modified with cysteamine. It was modified to increase detection sensitivity towards fumonisin

B1 and stability. Cysteamine can be easily connected to AuNPs because it has the thiol group. Thus, cysteamine attaches to the surface of AuNPs through strong Au-S covalent bond and $-NH_3^+$ group exposed on the surface of Cyst-AuNPs. The Cyst-AuNPs can be well-dispersed in the solution for long time because of electrostatic repulsion of $-NH_3^+$ on the surface of Cyst-AuNPs. The Cyst-AuNPs showed a wine-red color and an absorption peak at 520 nm like the synthesized AuNPs.

Fumonisin B1 contains many hydroxyl groups and aliphatic amines. Thus, it is expected that these groups will form hydrogen bonds with amine groups of cysteamine. Nevertheless, the aggregation of Cyst-AuNPs towards un-hydrolyzed fumonisin B1 are not satisfactory probably due to the steric interruption of large molecule of FB1. Therefore, FB1 was hydrolyzed in alkaline media to release its side chain off the native molecule and increase the hydroxyl group number. Hydrolyzed fumonisin B1 (HFB1) contains several hydroxyl groups (-OH). At pH 9, hydroxyl groups of HFB1 can interact with amine groups of cysteamine capped on AuNPs surface through hydrogen bonding as shown in Figure 3.4. The Cyst-AuNPs aggregated quickly, leading to the color change of the solution from wine-red to blue-gray, accompanied by the change in absorption peak which leads to a shift in absorption intensity to longer wavelength 645 nm.

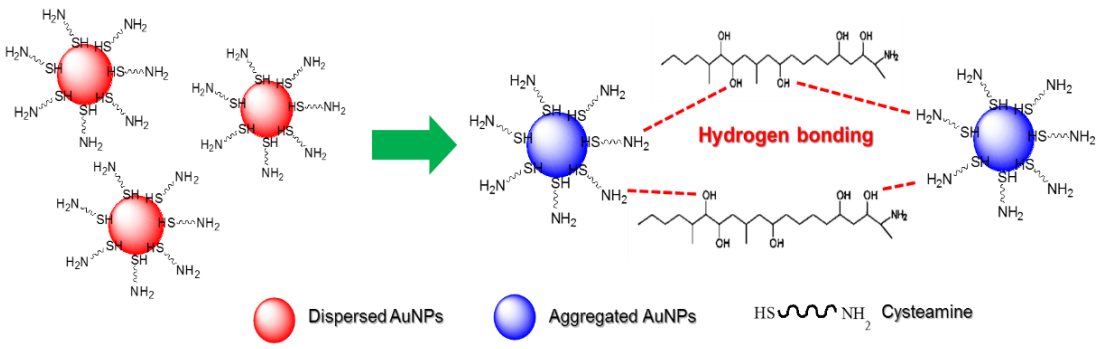

Figure 3.4 The schematic of the colorimetric detection strategy for hydrolyzed fumonisin B1 based on cysteamine modified with AuNPs.

3.3 Characterization

3.3.1 The UV-vis absorption behaviors of AuNPs

The absorption spectra of AuNPs, Cyst-AuNPs and the aggregation of Cyst-AuNPs are shown in Figure 3.5. The diluted AuNPs solution showed a maximum absorption spectrum at 520 nm (Figure 3.5a) with a wine-red color (Figure 3.5A). In addition, 0.01 µM of cysteamine was added to functionalized AuNPs (1:9) as shown in Figure 3.5b. The color of the Cyst-AuNPs solution remains red (Figure 3.5B), like the as-synthesized AuNPs solution. It indicated that the Cyst-AuNPs are well dispersed and stable.

After addition of 10 mg L^{-1} HFB1, the new maxima absorption band appeared at 645 nm and the intensity at 520 nm decreased as shown in Figure 3.5c. The color of solution changed from wine red to blue (Figure 3.5C), indicating that HFB1 induced Cyst-AuNPs to aggregate via hydrogen bonding (Figure 3.4).

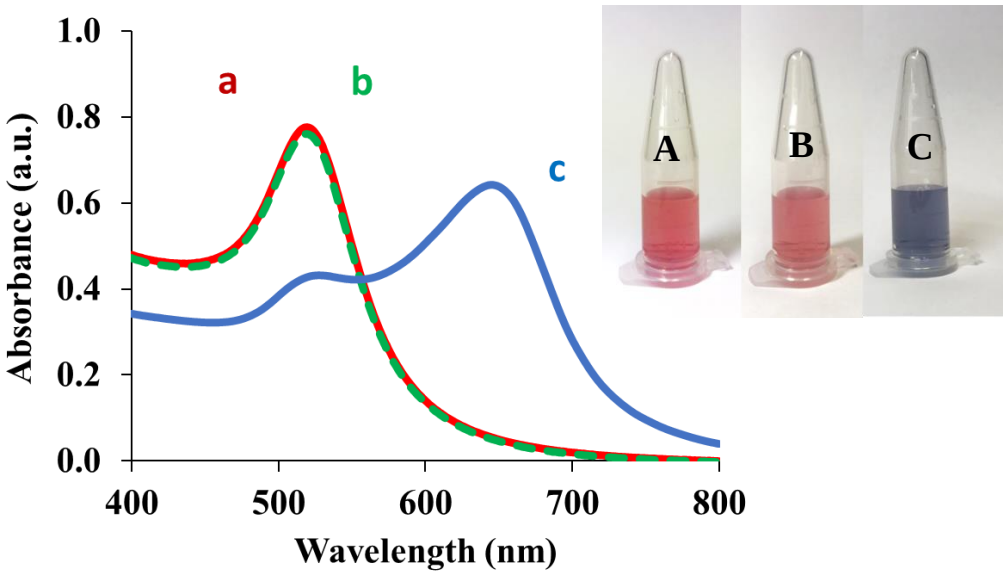

Figure 3.5 UV-Vis absorption spectra of (a) AuNPs, (b) Cyst-AuNPs and (c) aggregation of Cyst-AuNPs in the presence of 10 mg L^{-1} HFB1. Photographs of A, B and C correspond to a, b, and c spectrum, respectively.

3.3.2 The functional groups of modified AuNPs

The cysteamine functionalized AuNPs was confirmed by Fourier- transform infrared (FTIR) spectroscopy. The samples were prepared as mentioned in section 2.8.2.

To elucidate the modification of Cyst-AuNPs, FTIR investigations were carried out. In Figure 3.6A, the characteristic skeleton peaks of cysteamine were 3422 cm^{-1} (N-H), 3350 cm^{-1} (N-H), 2558 cm^{-1} (S-H). In Figure 3.6B, the peak that was originally at 2558 cm^{-1} (S-H) disappeared, indicating that SH group coordinates with the gold atoms on the surface of AuNPs, confirming the successful modification of cysteamine onto the surface of AuNPs via the SH group. This result was also in agreement with a previous report (Zhang et al., 2011).

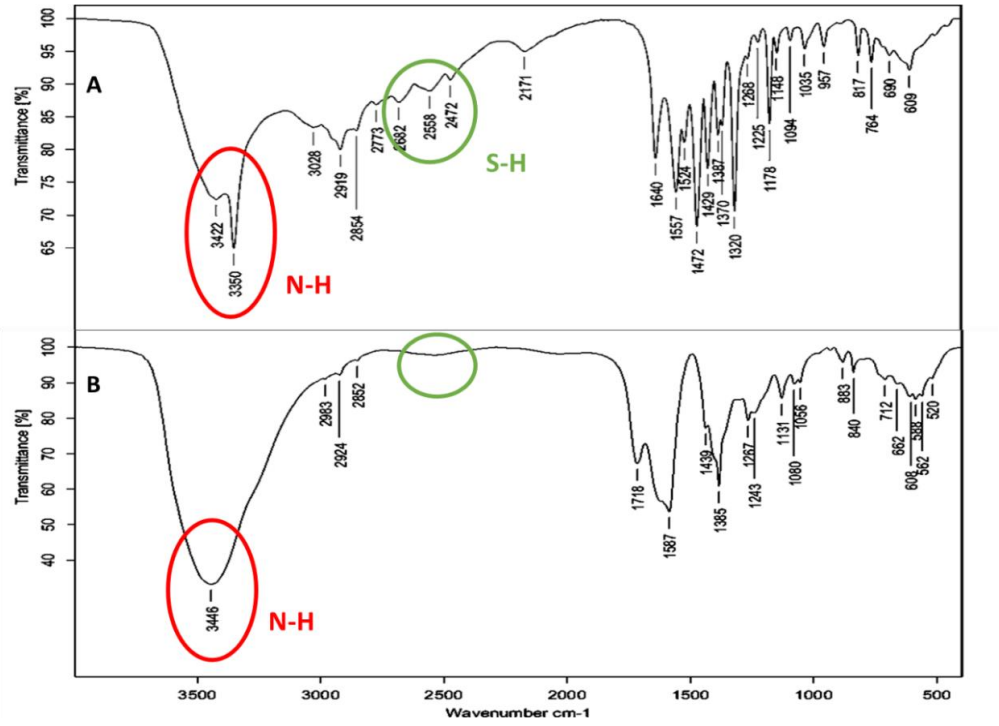

Figure 3.6 The FTIR spectra of (A) cysteamine and (B) cysteamine capped AuNPs.

3.3.3 The morphology of modified AuNPs

The morphology of the cysteamine capped gold nanoparticles surface was evaluated by transmission electron microscopy (TEM) technique. This technique is used to study the size and shape of Cyst-AuNPs and aggregated Cyst-AuNPs. Sample was prepared as described in section 2.8.3.

The TEM images of Cyst-AuNPs and Cyst-AuNPs in the presence of 10 mg L^{-1} HFB1 was measured at the magnitude of 100,000 times as shown in Figure 3.7. The Cyst-AuNPs were dispersed well in solution. Each AuNPs particle was spherical and mono-dispersed (Figure 3.7A). In contrast, Cyst-AuNPs rapidly aggregated in the presence of 10 mg L^{-1} HFB1, which can be observed that the particles are closely connected and spread all over (Figure 3.7B), confirming that fumonisin B1 induced Cyst-AuNPs to aggregation state. Hence, this probe is effective for the detection of fumonisin B1.

(A)

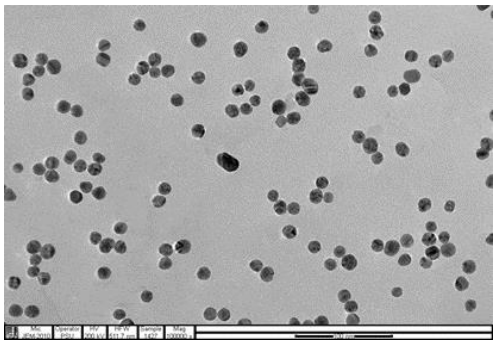

(B)

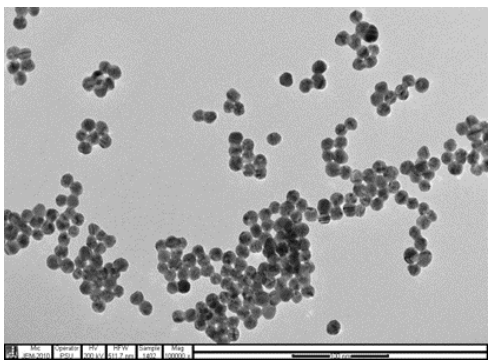

Figure 3.7 The TEM images of (A) Cyst-AuNPs and (B) aggregation of Cyst-AuNPs in the presence of 10 mg L^{-1} HFB1.

3.3.4 Particle size distribution of Cyst-AuNPs

The particles size distribution of Cyst-AuNPs and the aggregation of Cyst-AuNPs were determined by a zeta potential analyzer as shown in Figure 3.8. Sample preparation was performed as shown in section 2.8.5.

The lognormal distribution resultant of effective diameter (ED) of dispersed Cyst-AuNPs solution shows particles size of 13.6 ± 0.1 nm (Figure 3.8A), which was in good agreement with the histogram of particle size in Figure 3.3 with average particles size of 13.3 ± 1.0 nm. This confirmed that Cyst-AuNPs was successfully synthesized with results of particle size distribution, validating that obtained from TEM studies. Moreover, the Cyst-AuNPs in the presence of fumonisin B1 was aggregated, leading to the increased particle size as shown in Figure 3.8B, where it was demonstrated particles size distribution of 234.3 ± 3.7 nm. This also confirmed that hydrolyzed fumonisin B1 can induced Cyst-AuNPs to aggregation.

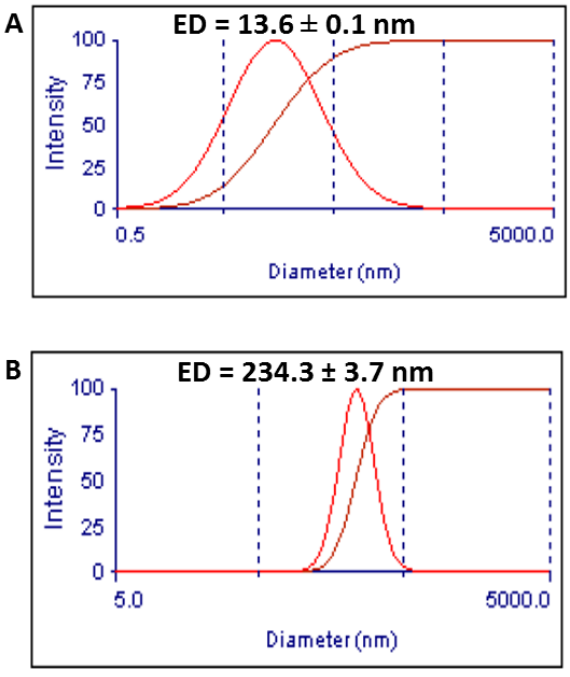

Figure 3.8 Lognormal distribution diagram of effective diameter (ED) of (A) Cyst-AuNPs and (B) the aggregation of Cyst-AuNPs in the presence of HFB1.

3.3.5 Zeta potential of Cyst-AuNPs

Zeta potential analysis is a technique for determining the surface charge of gold nanoparticles in solution. The magnitude of the zeta potential used for predicting the colloidal stability. Thus, the zeta potential of AuNPs, Cyst-AuNPs and the aggregation of Cyst-AuNPs were determined by zeta potential analyzer as shown in Figure 3.9. Sample preparation was performed as described in section 2.8.4.

We investigated the zeta potential of AuNPs, as shown in Figure 3.9. The AuNPs covered with citrate ion shows zeta potential of -28.19 ± 1.42 mV, confirming the electrostatic repulsion and stabilization provided by the negative charged citrate ion. However, the addition of cysteamine to the as-synthesized AuNPs would result in a facile replacement of the citrate ion on AuNPs surface through ligand exchange by the common (Au-S) covalent interaction. As a result, the AuNPs is more stable and has negative zeta potential value of -36.56 ± 1.32 mV. The addition of HFB1 to the functionalized AuNPs (Cyst-AuNPs) leads to decrease in the zeta potential value to -26.17 ± 0.40 mV, resulting from the interaction of the functional group of cysteamine and HFB1.

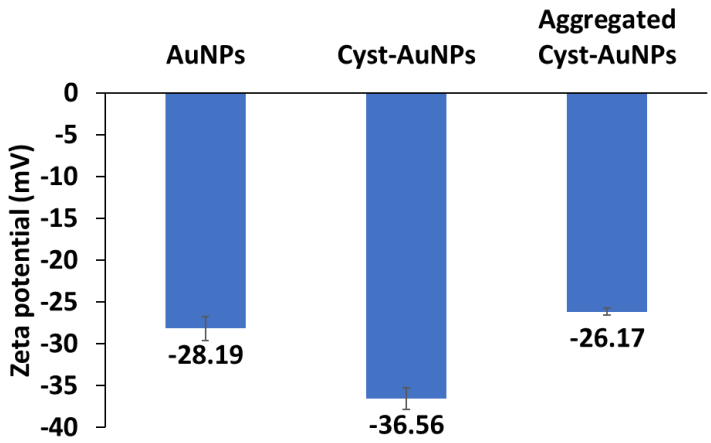

Figure 3.9 Zeta potential of AuNPs (-28.19 ± 1.42 mV), Cyst-AuNPs (-36.56 ± 1.32 mV) and aggregated Cyst-AuNPs (-26.17 ± 0.40 mV).

3.3.6 The stability of AuNPs

The stability of synthesized AuNPs was studied by recording the absorbance at 520 nm of AuNPs which was diluted 0.5-fold with ultrapure water. The absorbance was recorded by UV-Vis spectrophotometer, from one day after synthesis until 4 months for every 2 weeks.

Figure 3.10 shows the maximum absorbance at 520 nm of diluted AuNPs solution with an average absorbance of 0.66 ± 0.01. It was found that there was no significant difference of absorbance measurement during studied period. This result indicates the good stability of citrate capped AuNPs. In addition, this shows that the synthesized AuNPs can be kept in refrigerator up to 4 months without any loss of sensitivity.

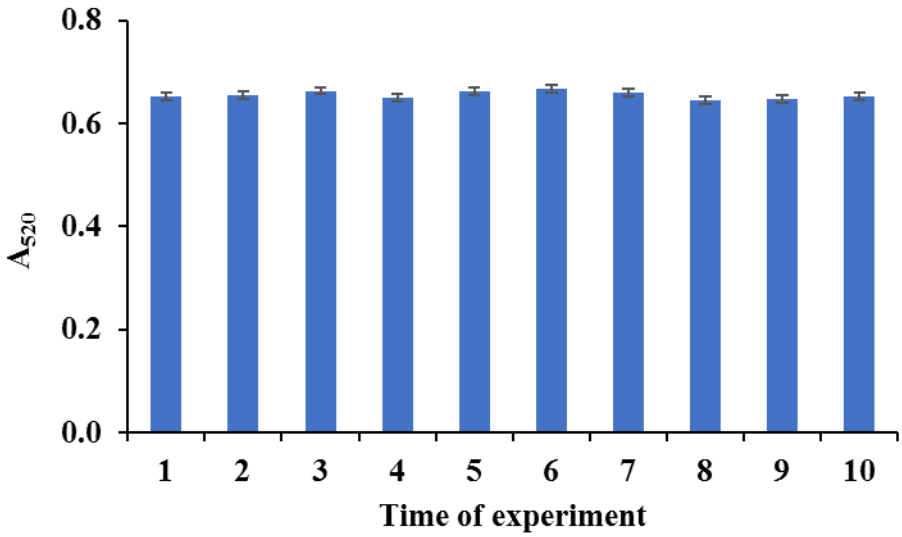

Figure 3.10 The absorbance intensity at 520 nm of diluted AuNPs solution at every two weeks for 4 months.

3.4 Optimization of parameters affecting the fumonisin B1 detection

To achieve the highest sensitivity of fumonisin B1 detection, three parts of optimization were performed including (i) optimization of cysteamine functionalized on AuNPs surface, (ii) optimization of alkaline hydrolysis and (iii) optimization of colorimetric detection based on Cyst-AuNPs.

3.4.1 Optimization of cysteamine functionalized on AuNPs surface

3.4.1.1 Effect of cysteamine concentration

Cysteamine was used as the capping agent since the amino group of cysteamine molecule contributes to the aggregation of AuNPs. Therefore, appropriate concentration of cysteamine in the colorimetric detection system was investigated. The concentration of cysteamine should be as high as possible but not to induce AuNPs aggregation. Figure 3.11 shows the effect of different concentrations of cysteamine added to AuNPs solution at room temperature. When the concentration of cysteamine increased to over 0.01 µM, the AuNPs can be aggregated, hence the suitable concentration of cysteamine at 0.01 µM was chosen for further experiments.

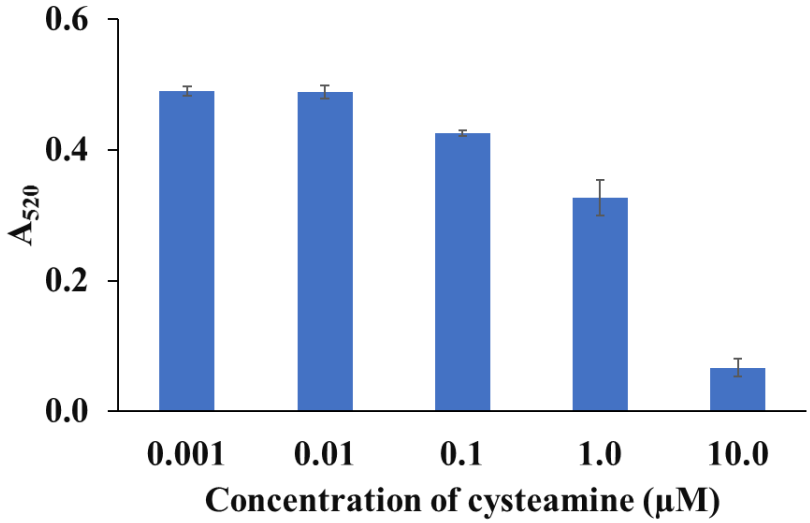

Figure 3.11 Effect of concentration of cysteamine for functionalized on AuNPs surface.

3.4.1.2 Reaction time of cysteamine binding to AuNPs

The effect of reaction time in the range of 5-20 minutes for cysteamine capped on AuNPs surface was performed by adding 0.01 µM cysteamine into AuNPs solution (AuNPs:cysteamine, 9:1). As seen in Figure 3.12, it was found that with longer time, color and absorbance of modified AuNPs was still constant. Thus, reaction time of 5 minutes was adopted in subsequent analysis.

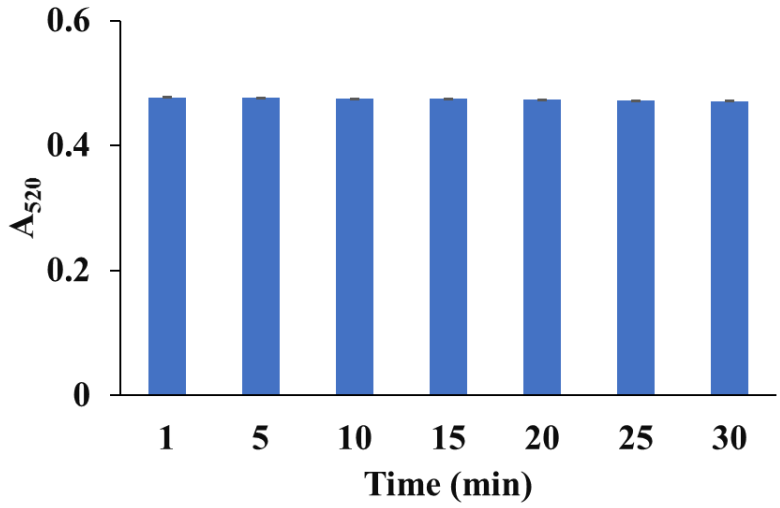

Figure 3.12 Effect of reaction time for functionalized cysteamine on AuNPs surface.

3.4.2 Optimization of alkaline hydrolysis

3.4.2.1 Effect of concentration of KOH for hydrolysis of fumonisin B1

Alkaline hydrolysis is a simple, natural process by which complex molecules can be broken down (Kaye et al., 2004). Free fumonisin forms including hidden esterified fumonisins as well as fumonisin covalently bound via carboxyl group to other substances present in food are easily hydrolyzed in alkaline media, releasing its side chain off the native molecule (Thacker, 2004).

In this work, potassium hydroxide (KOH) has been used as the hydrolysing agent. The concentration of KOH was investigated in the range of 0.5-1.3 M as shown in Figure 3.13. Furthermore, to confirm the performance of hydrolysis involving the percent conversion of FB1 to HFB1, liquid chromatography-tandem mass spectrometry (LC-MS/MS) was performed as shown in Table 3.1. Mass spectrum of parent FB1 and hydrolyzed product (HFB1) was shown in Figure 3.14. In Figure 3.12, the absorbance ratio (A_{645}/A_{520}) at 0.5 M KOH was very low as a result of poor aggregation of Cyst-AuNPs in the presence of HFB1. At this concentration, the % hydrolysis was calculated to be 91.6%. This confirmed that low concentration of KOH, resulted in less hydrolyzed product. The absorbance ratio became significantly increasing with increasing concentration of KOH from 0.7 to 1.3 M, leading to high aggregation of the Cyst-AuNPs. The % hydrolysis reached 100% at 1.0 and 1.3 M KOH, meaning that FB1 was completely transformed to HFB1. From the observation of solution color, the color of solution of 1.0 M KOH changed from wine-red to blue as well as significant change in the UV-Vis spectrum. The concentration from 1.0 M, complete hydrolysis of FB1 can be achieved. This showed that 1.0 M KOH was the minimum concentration that can completely hydrolyze FB1. However, high concentrations of KOH interfere with aggregated Cyst-AuNPs system that the blue color of the aggregated Cyst-AuNPs quickly disappeared. Thus, 1.0 M of KOH solution was chosen for next experiment.

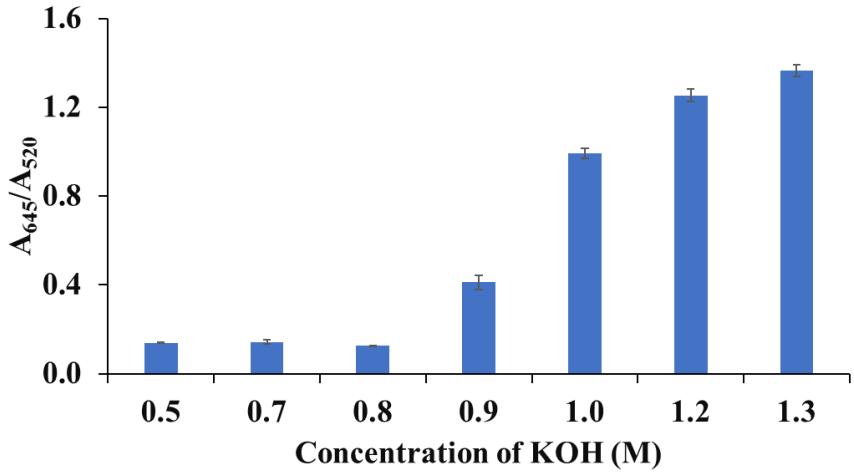

Figure 3. 13 Effect of concentration of potassium hydroxide for the hydrolysis of fumonisin B1.

Table 3.1 The efficiency of FB1 hydrolysis calculated from results of LC-MS/MS peak area.

Concentration of KOH (M)	LC-MS/MS peak area		% FB1 remaining	% Hydrolysis (Conversion of FB1 to HFB1) *
	FB1	HFB1		
0.5	214530	2546417	8.4	91.6
0.7	31910	2616560	1.2	98.8
1.0	10241	2614223	0.4	99.6
1.3	0	2600754	0.0	100.0

*Hydrolysis calculation; %Hydrolysis = (Peak area of HFB1/Total peak area) ×100

A

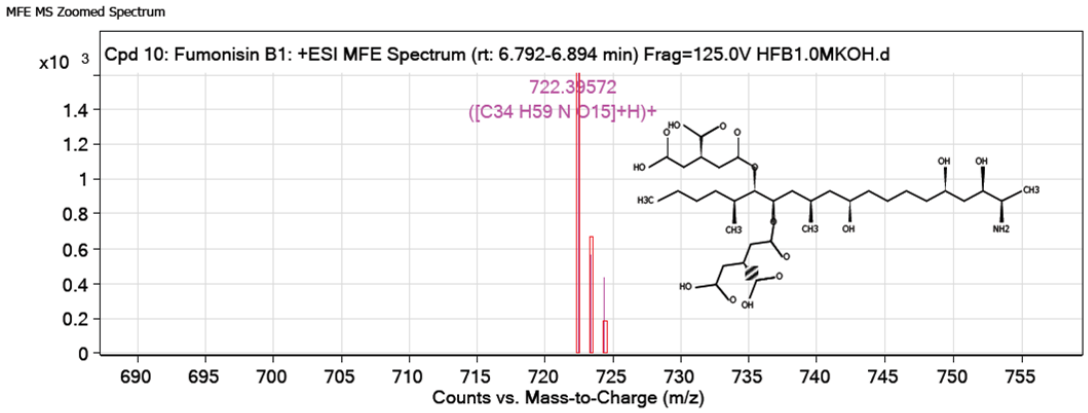

User Chromatogram Peak List

RT	Height	Height %	Area	Area %	Area Sum %	Base Peak m/z	Width
6.837	2150	100	10241	100	100	125.9859	0.063

B

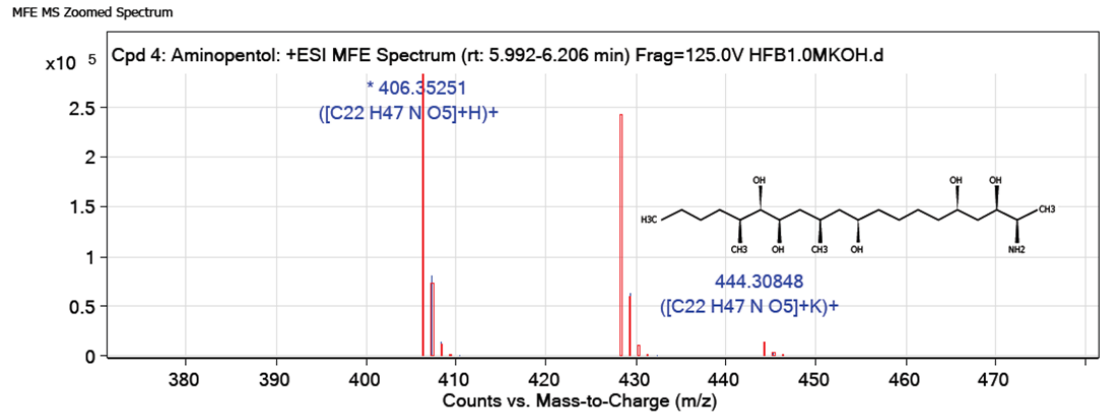

User Chromatogram Peak List

RT	Height	Height %	Area	Area %	Area Sum %	Base Peak m/z	Width
6.064	397615	100	2614223	100	100	406.35527	0.089

Figure 3.14 Mass spectra from LC-MS/MS of (A) fumonisin B1 and (B) hydrolyzed fumonisin B1 (HFB1) after hydrolysing fumonisin B1 with 1.0 M KOH.

3.4.2.2 Time of hydrolysis

The influence of hydrolysis time ranged from 10-100 min upon the interaction between 10 mg L^{-1} FB1 and 1.0 M KOH. As shown in Figure 3.15, it can be seen that the absorption ratio (A_{645}/A_{520}) increased from 10 to 60 min and was then stable from 60 to 100 min. This indicated that the hydrolysis was completed at 60 min. Thus, 60 min of hydrolysis time was chosen.

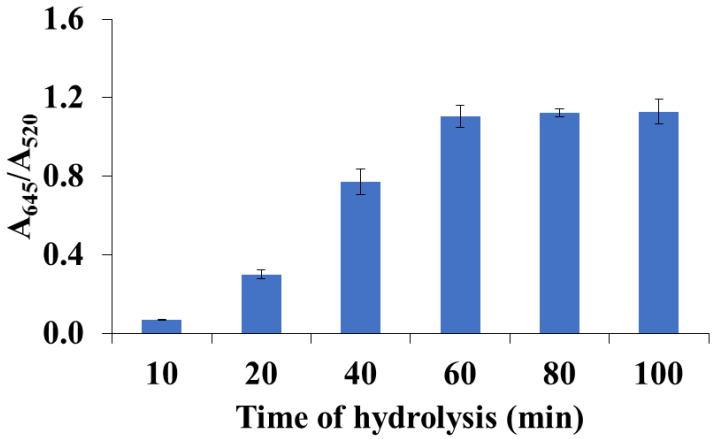

Figure 3.15 Effect of hydrolysis time for fumonisin B1.

3.4.2.3 Temperature of hydrolysis

Temperature is one of factors required for hydrolysis. The influence of hydrolysis temperature was investigated ranging from 30 to 90˚C. Figure 3.16 shows that when hydrolysis with low temperature, the structure of fumonisin B1 is less hydrolyzed. Thus, the aggregation of AuNPs occurs low level. When temperature was increased, the breakdown of the fumonisin B1 structure increases as seen from the increase in absorbance ratio until at 70˚C. Afterwards the absorbance ratio was stable. This indicated that the hydrolysis was completed at 70˚C. Thus, 70˚C of hydrolyzed temperature was chosen.

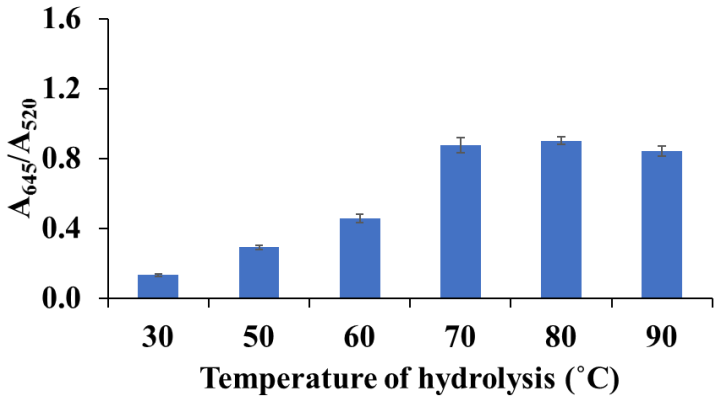

Figure 3.16 Effect of hydrolysis temperature on the hydrolysis of fumonisin B1.

3.4.3 Optimization of colorimetric detection based on Cyst-AuNPs

3.4.3.1 The effect of pH of Britton-Robinson buffer

pH value of reaction environment is one of critical factors towards achieving a highly sensitive detection strategy in Cyst-AuNPs based colorimetric methods. Hence, the pH values of the proposed assay was optimized from 3 to 12 using a 10 mM of Britton-Robinson buffer in the presence of 10 mg L^{-1} HFB1. As shown in Figure 3.17, the absorbance ratio increased as pH increased from 3 to 9, then decreased afterwards. This trend can be explained based on the structure of cysteamine capping agent on the modified AuNPs surface. At low pH, the exposed amine group (NH_2) of cysteamine was protonated and existed as a positively charged ligand (NH_3^+). This would decrease the ease of formation of hydrogen bonding (H-bonding) between Cyst-AuNPs and the hydrolyzed FB1. When the pH increased from 3 to 8, and 9 cysteamine changed to the deprotonated form (NH_2) (Oliva et al., 2018). Thus, this neutral form is very suitable for effective hydrogen bonding formation with the hydrolyzed fumonisin B. However, at higher pH 9, the response towards hydrolyzed fumonisin B1 decreased due to excessive basic media which may affect the stability of Cyst- AuNPs and hydrolyzed

fumonisin B1 and thus led to ineffective bonding. Consequently, pH 9 was selected in this work.

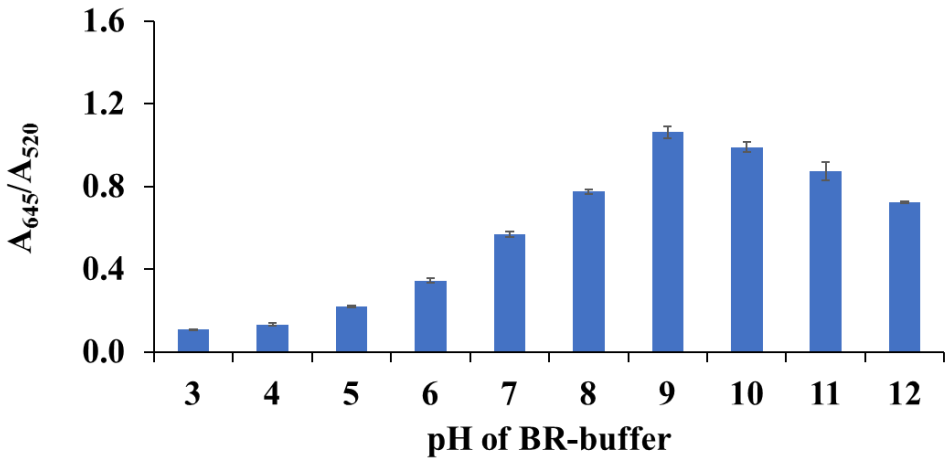

Figure 3.17 The absorbance ratio (A_{645}/A_{520}) of the Cyst-AuNPs under different pH of Britton-Robinson buffer on the colorimetric assay for fumonisin B1.

3.4.3.2 The concentration of Britton-Robinson buffer

The different type of buffer, *i. e.* phosphate, citrate, Britton- Robinson and acetate have been used in many reported (Souri et al., 2013). Britton- Robinson buffer was selected for further investigation due to their high solubility in water and high buffering capacity in the wide range from 3 to 12. The effect of ionic strength has been evaluated by changing the buffer concentration. As shown in Figure 3.18, the absorbance ratio (A_{645}/A_{520}) was found increased in proportion to the buffer concentration and reached maximum value at 10.0 mM buffer. The result presented that a buffer concentration of 50.0 mM led to increase of much ionic strength. Then Cyst-AuNPs was aggregated and blue color of solution disappeared quickly, resulting in an increase in the absorbance ratio. Thus, Britton- Robinson buffer solution at 10.0 mM was selected for further investigation.

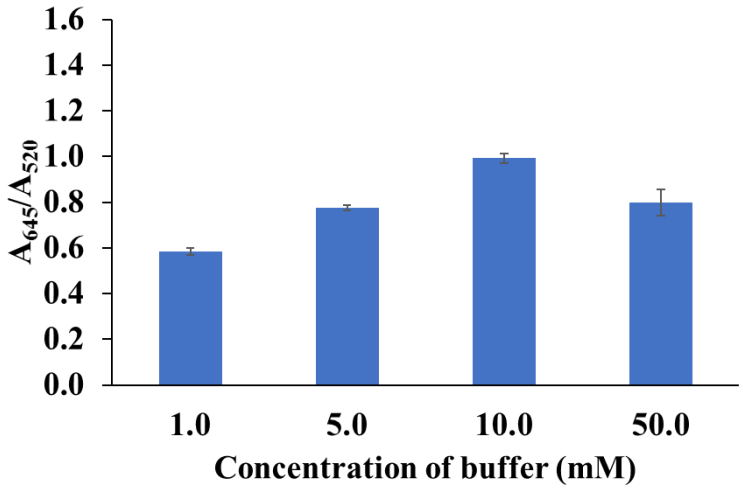

Figure 3.18 The absorbance ratio (A_{645}/A_{520}) of the Cyst-AuNPs under different concentration of Britton-Robinson buffer on the colorimetric assay for fumonisin B1.

3.5 Method validation for fumonisin B1 determination

3.5.1 Linearity of standard curve

Under optimized conditions, the different concentration of FB1 solutions in the range of 0.5-25.0 µg L^{-1} and 10.0 mM of Britton-Robinson buffer (pH 9) were added to Cyst-AuNPs solution. When the FB1 concentration was increased from 0.5-25.0 µg L^{-1}, the UV-Vis absorption changed. The absorbance at 645 nm increased and the peak at 520 nm decreased due to the transition from the dispersion state to aggregation state of Cyst-AuNPs as shown in Figure 3.19a. The absorbance ratio (A_{645}/A_{520}) curve tended to increase from 2.0 µg L^{-1} and was found stable at concentration 15.0 µg L^{-1} (Figure 3.19b), therefore linearity range was obtained in the range of 2.0-10.0 µg L^{-1}.

The linearity of developed sensor based on UV-Vis measurement was in the range 2.0-10.0 µg L^{-1} with a linear equation of $y = 0.1083x - 0.0891$ and a coefficient of determination (R^2) of 0.9994 as shown in Figure 3.20b. The color of solution changed from red to purple, and finally to blue-gray as shown in Figure 3.20a. Thus, this sensor

shows a good linearity with the color transition easily observed by naked eyes from blank until constant color of solution.

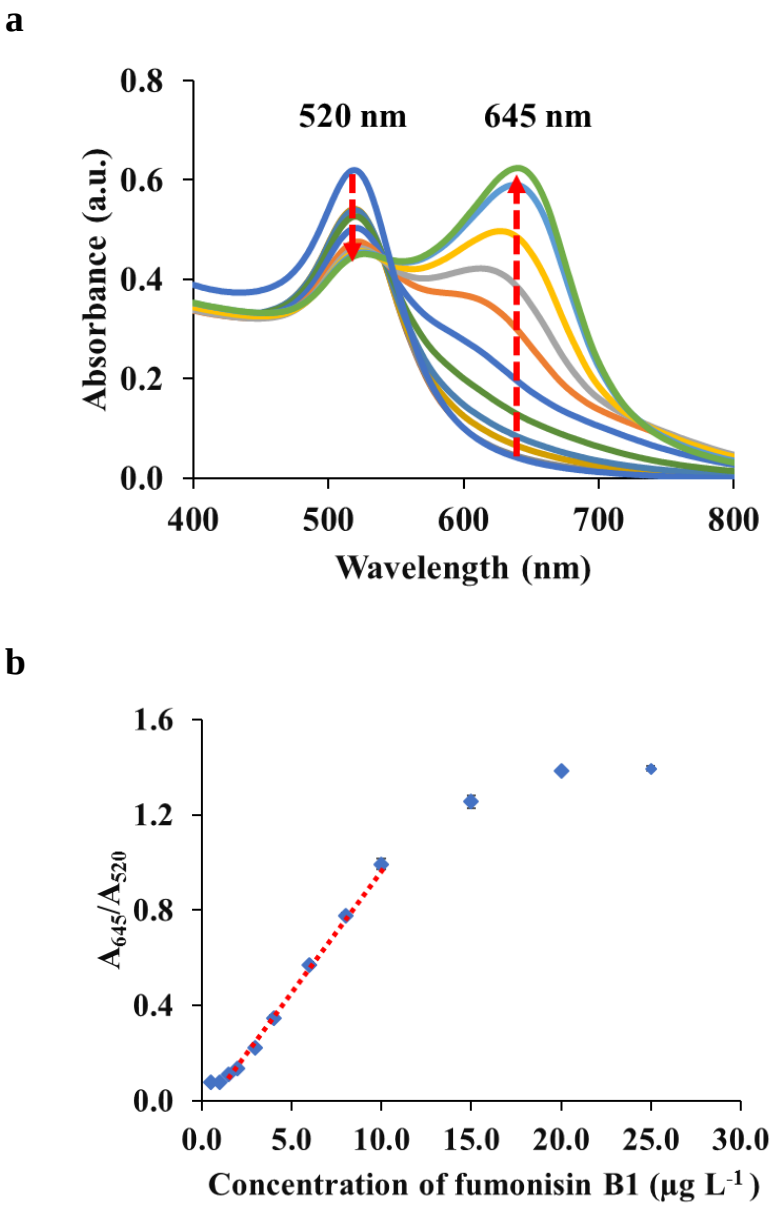

Figure 3.19 (a) UV-Vis absorption spectra of Cyst-AuNPs relating to the different concentration of FB1. (b) Plot of absorbance ratio (A_{645}/A_{520}) against different concentrations of FB1 in the range of 0.5-25.0 µg L^{-1}.

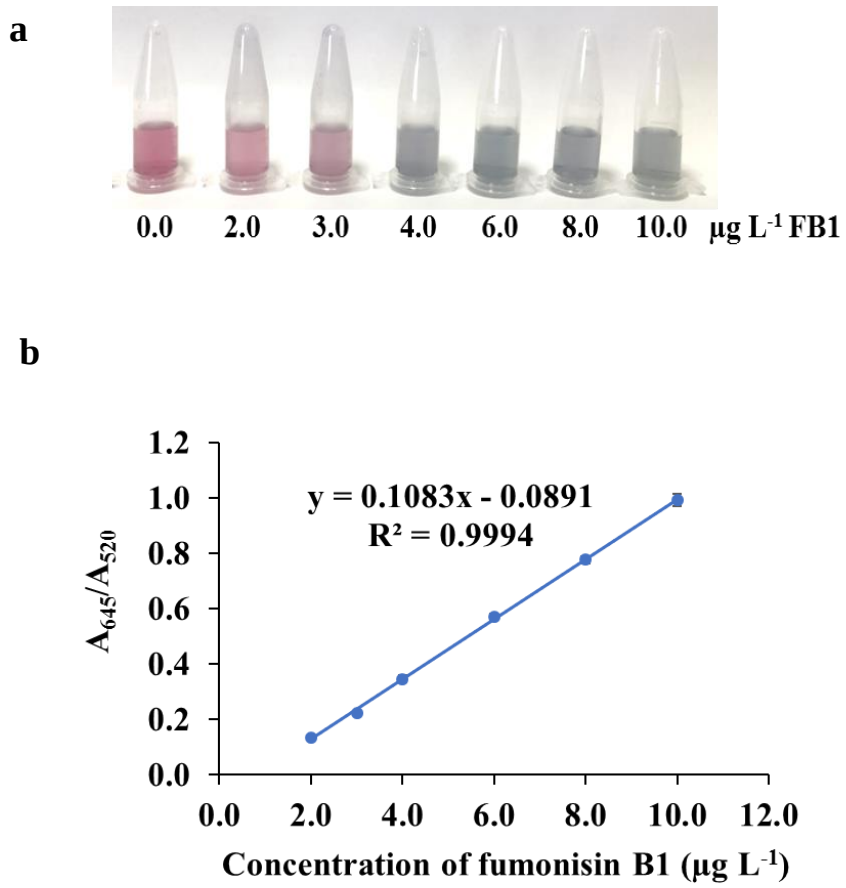

Figure 3.20 (a) Color of solution of Cyst-AuNPs based on the different concentrations of fumonisin B1. The optimum condition: 600 µL of Cyst- AuNPs, 200 µL of 10 mM BR-buffer. (b) The linear calibration curve in the range of 2.0-10.0 µg L^{-1} of fumonisin B1.

3.5.2 Limit of detection (LOD) and limit of quantification (LOQ)

The calculation of LOD and LOQ were performed by the equation 3.3 σ/*s* and 10 σ/*s*, respectively, where σ is the standard deviation of the response which is estimated by the y-residual standard deviation of the regression line and *s* is the slope of the calibration curve (ICH,1996). Under the linear equation of standard calibration curve of y = 0.1083x - 0.0891, LOD and LOQ was 0.84 and 2.55 µg L^{-1}, respectively.

3.5.3 Matrix effect

The matrix effect was investigated by using a standard addition curve. Figure 3.21 shows the plot between the ratio A_{645}/A_{520} (y axis) *versus* FB1 concentrations (x axis) in the range of 2.0-10.0 µg kg^{-1}. The curve was linear over the range of 2.0-8.0 µg kg^{-1} with an equation of y = 0.0966x + 0.1244 and a correlation coefficient (R^2) of 0.9904 as shown in Figure 3.21a.

From Figure 3.21, the sensitivity of standard addition curve (a) was significantly different from that of standard curve (b) ($p < 0.05$), indicating that the matrix had effect on analysis of fumonisin B1 in corn samples**.** Therefore, the standard addition curve was used for accurate determination of fumonisin B1 in corn samples.

The limit of detection (LOD) and limit of quantification (LOQ) from an equation of y = 0.0966x + 0.1244 were found to be 0.90 µg kg^{-1} and 2.74 µg kg^{-1}, respectively, based on the equation 3.3 σ/s and 10 σ/s, respectively (ICH, 1996).

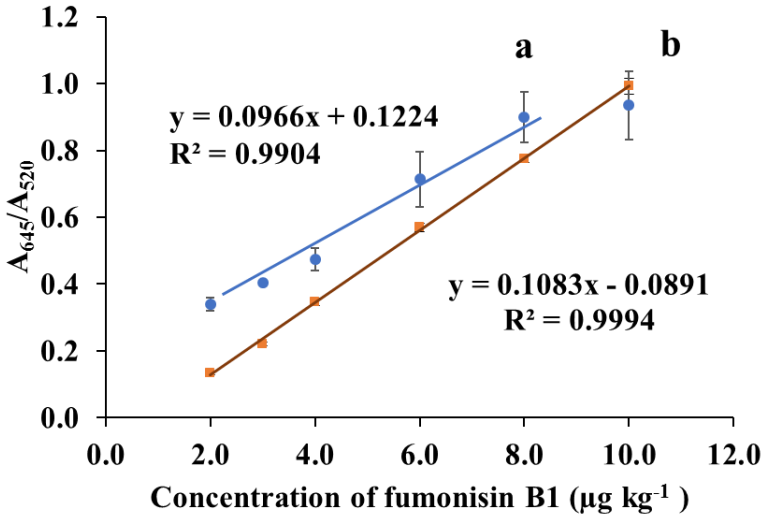

Figure 3.21 (a) The standard addition curve and (b) the standard calibration curve for fumonisin B1.

3.5.4 Accuracy

The accuracy of developed method was investigated by recovery study which was determined by spiking 2.0, 4.0 and 6.0 μg kg^{-1} into corn samples. Table 3.2 shows recovery values of three concentrations levels of FB1. The satisfactory recoveries were 93.1 to 99.3% with RSDs less than 5.0% (n = 3). These recoveries were acceptable according to standard recovery of 60-115% reported by AOAC standard method (AOAC, 2012). This result indicates that this sensor is effective for determination of fumonisin B1.

Table 3.2 Recovery results of fumonisin B1 in the composite corn samples

Concentration of fumonisin B1 (μg kg^{-1})		**Recovery (%)**	**RSD (%, n = 3)**
Added	**Found (mean ± SD)**	**(mean ± SD)**	
0.00	Not detected	–	–
2.00	1.93 ± 0.06	93.1 ± 2.01	2.2
4.00	4.00 ± 0.13	99.3 ± 4.05	4.1
6.00	5.96 ± 0.05	98.0 ± 3.37	3.4

3.5.5 Precision

The precision of Cyst-AuNPs assay for fumonisin B1 was investigated by analyzing three concentrations of fumonisin B1 (2.0, 6.0 and 10.0 μg kg^{-1}) under five different times in the same day for intra-day precision and same concentrations were determined on 5 days for inter-day precision. The results as shown in Table 3.3 shows that the colorimetric method for FB1 detection demonstrated acceptable intra- and inter-day precision with RSD ranging between 1.0-5.6% and 3.6-6.1% respectively. These precisions were in the AOAC standard precision (repeatability) which is not more than 21% for 10 μg kg^{-1} analyte concentration (AOAC, 2012).

Table 3.3 Precisions of colorimetric detection at three concentration levels of FB1.

Concentration (μg L^{-1})	**Intra-day precision (% RSD, n = 5)**	**Inter-day precision (% RSD, n = 5)**
2	1.0	6.1
6	4.4	5.3
10	5.6	3.6

3.6 Selectivity

The composition of corn samples was studied from previous reports (Batal et al., 2012; H. & Victor, 2014; FAO, 2010). They reported that the composition in corns includes, carbohydrate, protein, minerals, fat and mycotoxin. However, some compositions such as carbohydrate, fat and phospholipid were removed in clean-up step with Oasis PRiME HLB cartridge (Young & Tran, 2017). Therefore, in this work, we are interested in studying especially mycotoxins which probably interfere the selectivity of fumonisin B1.

The effect of other mycotoxins which can be found in corn samples were investigated. Other mycotoxins including aflatoxin, zearalenone, citrinin and patulin were studied with 3 replicates under the optimum conditions. The absorbance ratio (A_{645}/A_{520}) and color detection were compared between 6.0 μg L^{-1} of fumonisin B1, 12.0 μg L^{-1} of each mycotoxin (aflatoxin, zearalenone, citrinin and patulin), and the mixture of 6.0 μg L^{-1} of fumonisin B1 and 12.0 μg L^{-1} of aflatoxin, zearalenone, citrinin and patulin.

The selectivity of fumonisin B1 was reported in terms of the absorbance ratio (A_{645}/A_{520}) and color detection in Figure 3.22a and Figure 3.22b, respectively. Figure 3.22 showed that our colorimetric sensor exhibited a high sensitivity for fumonisin B1 compared to other mycotoxins. This result shows the correlation with color changes of

Cyst-AuNPs. The other mycotoxins did not induce Cyst-AuNPs aggregation and the color of solution remained wine red probably owing to different structure of mycotoxin. Fumonisin B1 is an aliphatic compound, while other mycotoxins are of aromatic structures Therefore, other mycotoxins are difficult to hydrolyze, resulting no aggregation with Cyst-AuNPs. This indicated that this sensor is high selectivity for fumonisin B1 with hydrolysis process.

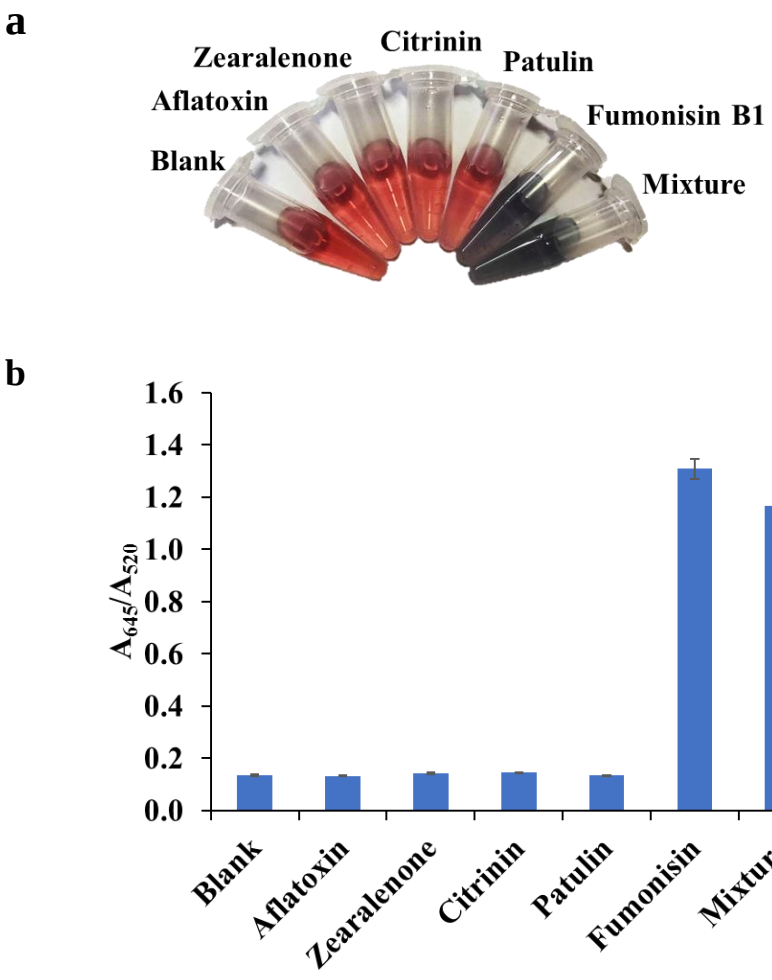

Figure 3.22 (a) The photograph of the corresponding detection for mycotoxins. (b) Selectivity of fumonisin detection. Absorbance ratio response (A_{645}/A_{520}) of the proposed sensor for 6.0 µg L^{-1} fumonisin B1 was plotted against the 12.0 µg L^{-1} of other mycotoxin (aflatoxin, zearalenone, citrinin, patulin) and the mixture of fumonisin B1 and other mycotoxins.

3.7 Application of the developed method to corn samples

Four corn kernel samples were collected randomly from the market in Songkhla province, Thailand and the two samples of ground corns were supplied by the National Corn and Sorghum Research Center (Bangkok, Thailand). The fumonisin B1 contamination of corn samples were determined under our developed method.

The determination of fumonisin B1 in corn samples was shown in Table 3.4 by our method. It was found that fumonisin B1 was not detected in any selected samples because it may be caused by the concentration of fumonisin B1 that is less contaminated than the limit of detection of the method. To confirm our proposed assay, high-performance liquid chromatography with fluorescence detector (HPLC- FLD) was applied (Table 3.4). It can be seen that fumonisin B1 were not found in the corn sample as well as our method. These results confirmed that the developed method can be applied for the analysis of fumonisin B1 in real samples.

Table 3.4 Comparison with the proposed colorimetric detection and HPLC-FLD.

Sample	Sample picture	Colorimetric assay based on Cyst-AuNPs (μg kg^{-1}, n = 3)	HPLC-FLD (μg kg^{-1}, n = 3)
SK1		Not detected	Not detected
SK2		Not detected	Not detected
SK3		Not detected	Not detected
SK4		Not detected	Not detected
BKK1		Not detected	Not detected
BKK2		Not detected	Not detected

3.8 Comparison of the developed method with other reported analytical methods

The performance of the developed method was compared with other previously reported method as presented in Table 3.5. Our method provides 223, 5 and 17 times lower LOD compared to ELISA (Coronel et al., 2016), electrochemical immunoassay (Kadir & Tothill, 2010; Lu et al., 2016) and colorimetric immunoassay (Chen et al., 2018; Ling et al., 2015), respectively. Additionally, the linear range of the proposed method is within the ranges reported by other methods (Coronel et al., 2016; Gazzotti et al., 2009; Kadir & Tothill, 2010; Ling et al., 2015). Overall, these results confirmed that our method for fumonisin B1 detection, based on aggregation of Cyst-AuNPs was more sensitive, efficient and could be applied in corn samples.

Table 3.5 Comparison of the present method with other methods for the detection of fumonisin B1.

Method	Sample type	Linear range	LOD	References
HPLC-FLD	Maize, gluten meal	3-8000 μg kg^{-1}	1 μg kg^{-1}	Coronel et al., (2016)
ELISA	Maize, gluten meal	250-6000 μg kg^{-1}	200 μg kg^{-1}	Coronel et al., (2016)
LC-MS/MS	Bovine milk	0.1-10.0 μg kg^{-1}	0.003 μg kg^{-1}	Gazzotti et al., (2009)
Electrochemical immunosensor	Corn	1-1000 μg L^{-1}	5 μg L^{-1}	Kadir & Tothill, (2010)
Electrochemical immunosensor	Corn	200-4500 μg L^{-1}	4.2 μg L^{-1}	Lu et al., (2016)
Colorimetric immunoassay	Corn	3.125-25 μg L^{-1}	12.5 μg L^{-1}	Chen et al., (2018)
Colorimetric immunostrip	Corn	2.5-10 μg L^{-1}	2.5 μg L^{-1}	Ling et al., (2015)
Colorimetric detection	Corn	2-8 μg kg^{-1}	0.9 μg kg^{-1}	This work

HPLC-FLD, High performance liquid chromatography-fluorescence detection; ELISA, Enzyme linked immunosorbent assay;

LC-MS/MS, Liquid chromatography-tandem mass spectrometry

CHAPTER 4

CONCLUSIONS

4.1 Conclusions

4.1.1 The synthesis of gold nanoparticles (AuNPs)

Gold nanoparticles (AuNPs) was successfully synthesized by reduction of chloroauric acid ($HAuCl_4$) with a reducing agent (trisodium citrate dihydrate). The solution color changes from yellow to wine red. The wine red colloidal solution of diluted AuNPs (0.5-fold) showed a maximum absorbance of 0.66 with the extinction coefficient for 13 nm AuNPs of about 2.70×10^8 M^{-1} cm^{-1} at 520 nm. The concentration of AuNPs was about 4.7 nM. Moreover, the size distribution of AuNPs was 13.3 ± 1.0 nm which agreed with previous reports. Therefore, the synthesis of AuNPs has been confirmed to be successful.

4.1.2 Proposed sensing mechanism

Citrate-stabilized AuNPs was modified with cysteamine. At pH 9, hydroxyl groups of HFB1 can interact with amine groups of cysteamine capped on AuNPs surface through hydrogen bonding. The Cyst-AuNPs aggregated quickly, leading to the color change of the solution from wine-red (dispersion state) to blue-gray (aggregation state), accompanied by the change in absorption peak, which led to a shift absorption intensity to longer wavelength 645 nm.

4.1.3 Characterization

The successfully modification of cysteamine onto the surface of AuNPs via the SH group was observed by FTIR. This result was also in agreement with previous reports (Zhang et al., 2011).

The TEM images of Cyst-AuNPs shows spherical mono-disperse colloidal solution. In the presence of 10 mg L^{-1} HFB1, Cyst-AuNPs was aggregated and the particles are closely connected and spread all over. Moreover, the particles size distribution of Cyst-AuNPs and the aggregation of Cyst-AuNPs were 13.6 ± 0.1 nm and 234.3 ± 3.7 nm, respectively by zeta potential analyzer (size analysis).

The zeta potential of AuNPs provided negative charge of citrate ion. After addition of cysteamine, zeta potential increased due to the better stability of AuNPs. Then, the addition of HFB1 to Cyst-AuNPs led to decrease in the zeta potential value, resulting from the interaction of the functional group of cysteamine and HFB1.

4.1.4 Optimization of parameters affecting the fumonisin B1 sensor

Optimization of conditions for fumonisin B1 detection was performed by 3 parts

1) Optimization of cysteamine functionalized on AuNPs surface

Cysteamine concentration was optimized to use for functionalized AuNPs surface. The concentration of cysteamine should be as high as possible, without inducing AuNPs aggregations. Thus, 0.01 µM of cysteamine was completely modified on AuNPs surface with 5 min for reaction time.

2) Optimization of alkaline hydrolysis

1.0 M of potassium hydroxide (KOH) was chosen to hydrolyze FB1, resulting in complete transformation of FB1 to HFB1 that was in agreement of LC-MS/MS confirmation. This concentration of KOH was suitable and not interfere with Cyst-AuNPs system.

In order to provide the most efficient hydrolysis, therefore, effect of time and temperature are also studied. From results, it was found that hydrolysis time of 60 min and hydrolysis temperature of 70˚C were suitable for the hydrolysis of FB1.

3) Optimization of colorimetric detection based on Cyst-AuNPs

The optimum pH of Britton-Robinson buffer in the presence of 10.0 mg L^{-1} HFB was 9 since cysteamine was changed to the deprotonated form (NH_2) at high pH

(Oliva et al., 2018). Thus, this neutral form is very suitable for effective hydrogen bonding formation with the hydrolyzed fumonisin B1. Moreover, the concentration of Briton-Robinson buffer of 10.0 mM was selected because this concentration provided the maximum absorbance ratio value.

4.1.5 Method validation for fumonisin B1 determination

Under optimized conditions, the developed method provides very good linear curve for FB1 ($y = 0.1083x - 0.0891$) in the range of 2.0-10.0 μg L^{-1} with satisfactory correlation coefficient (R^2) of 0.9994. The limit of detection (LOD) and limit of quantification (LOQ) were 0.84 and 2.55 μg L^{-1}, respectively. The satisfactory recoveries of spiking the FB1 concentrations were good ranging from 93.1 to 99.3% with RSDs less than 5.0% (n = 3). The precisions of Cyst-AuNPs assay for FB1 demonstrated intra- and inter-day as RSD ranged between 1.0-5.6% and 3.6-6.1% respectively. These recoveries and precisions were acceptable within the range referred to in AOAC standard method.

The matrix effect was investigated by using a standard addition curve in the range of 2.0-10.0 μg kg^{-1}. The standard addition curve was linear over the range of 2.0-8.0 μg kg^{-1} with an equation of $y = 0.0966x + 0.1224$ and R^2 of 0.9904. LOD and LOQ were found to be 0.90 and 2.74 μg kg^{-1}, respectively.

4.1.6 Selectivity

The other mycotoxins including aflatoxin, zearalenone, citrinin and patulin which can be found in corn samples were studied by comparing the absorbance ratio (A_{645}/A_{520}) and color detection was compared between 6.0 μg $L^{-1}$of FB1, 12.0 μg L^{-1} of each mycotoxin and the mixture of 6.0 μg L^{-1} of FB1 and 12.0 μg L^{-1} of other mycotoxins.

Our colorimetric sensor exhibited a high sensitivity for fumonisin B1 with other mycotoxins. The other mycotoxins were not induced Cyst-AuNPs to aggregation probably because it is difficult to hydrolyze aromatic structure under optimum

conditions. Thus, this sensor is high selectivity for fumonisin B1 with hydrolysis process.

4.1.7 Application of the developed method to corn samples

The determination of fumonisin B1 in corn samples which were randomly sampled from the market in Songkhla and Bangkok was determined by our sensor and compared with HPLC-FLD. Both techniques showed that FB1 were not found in any selected samples. These results confirmed that the developed method can be applied for the analysis of fumonisin B1 in real samples.

4.1.8 Comparison of the developed method with other reported analytical methods

Our method provides 223, 5 and 17 times lower LOD compared to ELISA, electrochemical and colorimetric immunoassay, respectively. Additionally, the linear range of the proposed method are within the ranges reported by other methods. Overall, these results confirmed that our method for fumonisin B1 based on aggregation of Cyst-AuNPs was more sensitive, efficient and can be applied in corn samples.

In conclusion, a robust colorimetric detection of fumonisin B1 based on hydrolyzed product induced aggregation of cysteamine functionalized gold nanoparticles was established. The aggregation of Cyst-AuNPs was marked with a changed in color (wine-red to blue-gray) that can be observed by the naked eyes and measured by UV-Vis spectrophotometry. It was also simple, highly sensitive and selective detection method. This work present low LOD and LOQ with satisfactory recoveries and precisions. Our developed method was suitable for detection of fumonisin B1 in corn samples.

4.2 Recommendations

To make our sensor more rapid analysis, the extraction and clean-up method of corn samples is next research focus.

References

Ajdari, N., Vyas, C., Bogan, S. L., Lwaleed, B.A., Cousin, B. G. (2017). Gold nanoparticle interactions in human blood: a model evaluation. Nanomedicine: Nanotechnology, Biology, and Medicine, 13(4), 1531-1542.

Akhond, M, Absalan, G., Ershadifar, H. (2015). Highly sensitive colorimetric determination of amoxicillin in pharmaceutical formulations based on induced aggregation of gold nanoparticles. Spectrochimica Acta Part A: Molecular and Biomolecular Spectroscopy, 143, 223-229.

AOAC. (2012). Guidelines for Standard Method Performance Requirements. Official Methods of Analysis of AOAC International, Appendix F, 1-17. www.eoma.aoac.org/app_f.pdf, accessed 07.01.2019.

AZoNano. (2013). Gold nanoparticles - properties, applications. https://www.azonano.com/article.aspx, accessed 07.01.2019.

Barna-Vetro, I., Szabó, E., Fazekas, B., Solti, L. (2000). Development of a sensitive ELISA for the determination of fumonisin B1 in cereals. Journal of Agricultural and Food Chemistry, 48(7), 2821-2825.

Batal, A. B., Dale, N. M., Saha, U. K. (2010). Mineral composition of corn and soybean meal, 361-364.

Bryla, M., Roszko, M., Szymczyk, K., Jedrzejczak, R., Obiedziński, M. W. (2016). Fumonisins and their masked forms in maize products. Food Control, 59, 619-627.

Chen, X., Liang, Y., Zhang, W., Leng, Y., Xiong, Y. (2018). A colorimetric immunoassay based on glucose oxidase-induced AuNP aggregation for the detection of fumonisin B1. Talanta, 186, 29-35.

Chen, Z., Wang, Z., Chen, X. (2013). Chitosan-capped gold nanoparticles for selective and colorimetric sensing of heparin. Journal of Nanoparticle Research, 15, 1930-1939.

Coronel, M. B., Vicente, S., Resnik, S. L., Alzamora, S. M., Pacin, A. (2016). Fumonisins in maize and gluten meal analysed in Argentinean wet milling industrial plants by ELISA compared with HPLC-FLD method. Food Control, 67, 285-291.

Cuadros-rodr, L., Bagur-gonz, M. G., Mercedes, S., Gonz, A., Antonio, M. G. (2007). Principles of analytical calibration / quantification for the separation sciences. Journal of Chromatography A, 1158, 33-46.

FAMIC. (2008). Fumonisin; Analysis method. http://www.famic.go.jp/ffis/oie/obj/m11- fumonisin.pdf, accessed 12.02.2019.

Food and Agriculture Organization of the United Nations (FAO). (1992). Maize in human nutrition. http://www.fao.org/3/T0395E/T0395E03.htm#20chemical%20composition, accessed 02.03.2019.

De Freitas, L. F., Henrique, G., & Varca, C. (2018). An Overview of the Synthesis of Gold Nanoparticles Using Radiation Technologies. Nanomaterials, 8(11), 939-961.

Garcia, P. L., Buffoni, E., Gomes, F. P., Luis, J., Quero, V. (2011). Analytical Method Validation. InTech, 1-19.

Gazzotti, T., Lugoboni, B., Zironi, E., Barbarossa, A., Serraino, A., Pagliuca, G. (2009). Determination of fumonisin B1 in bovine milk by LC-MS/MS. Food Control, 20(12), 1171-1174.

Gelderblom, W. C. A., Marasas, W. F. O., Vleggaar, R., Thiel, P. G., Cawood, M. E. (1992). Fumonisins: Isolation, chemical characterization and biological effects. Mycopathologia, 117(1-2), 11-16.

H., A. S., Victor, I. A. (2014). Comparison of chemical composition, functional properties and amino acids composition of quality protein maize and common maize (Zea may L). African Journal of Food Science and Technology, 5(3), 81-89.

International Agency for Research on Cancer (IARC). (2000). Some naturally occurring substances: food items and constituents, heterocyclic aromatic amines and mycotoxin. 56.

International Conference on Harmonisation of Technical Requirements for Registration of Pharmaceuticals for Human Use (ICH). (1996). Q2B Validation of analytical procedure: Methodology. ICH-Q2B, 1-10.

Kadir, M. K. A., Tothill, I. E. (2010). Development of an electrochemical immuno sensor for fumonisins detection in foods. Toxins, 2(4), 382-398.

Kaye, G., Weber, P., Wetzel, W. (2004). The Alkaline Hydrolysis Process. ALN Magazine (article posted 1st of September 2004).

Kong, S., Liao, M., Gu, Y., Li, N., Wu, P., Zhang, T., He, H. (2016). Colorimetric recognition of pazu floxacin mesilate based on the aggregation of gold nanoparticles. Spectrochimica Acta Part A: Molecular and Biomolecular Spectroscopy 157, 244-250.

Krska, R., Schuhmacher, R., Grasserbauer, M. and Scott, P. M. (1996). Determination of the Fusarium mycotoxin beauvericin at μg/kg levels in corn by high-performance liquid chromatography with diode-array detection. Journal of Chromatography A, 746(2), 233-238.

Kumar, A., Pandey, S., Nerthigan, Y., Swaminathan, N., Wu, H. (2018). Analytica Chimica Acta Aggregation of cysteamine-capped gold nanoparticles in presence of ATP as an analytical tool for rapid detection of creatine kinase (CK-MM). Analytica Chimica Acta, 1024, 161-168.

Li, C., Wu, Y. L., Yang, T., Huang-Fu, W. G. (2012). Rapid determination of fumonisins B1 and B2 in corn by liquid chromatography-tandem mass spectrometry with ultrasonic extraction. Journal of Chromatographic Science, 50(1), 57-63.

Ling, S., Wang, R., Gu, X., Wen, C., Chen, L., Chen, Z., Wang, S. (2015). Rapid detection of fumonisin B1 using a colloidal gold immunoassay strip test in corn samples. Toxicon, 108, 210-215.

Liu, G., Lu, M., Huang, X., Li, T., Xu, D. (2018). Application of gold-nanoparticle colorimetric sensing to rapid food safety screening. Sensors (Switzerland), 18(12), 1-16.

Liu, G., Wang, S., Yang, X., Li, T., She, Y., Wang, J., Shao, H. (2016). Colorimetric sensing of atrazine in rice samples using cysteamine functionalized gold nanoparticles after solid phase extraction. Analytical Methods, 1, 52-56.

Lu, L., Seenivasan, R., Wang, Y. C., Yu, J. H., Gunasekaran, S. (2016). An electrochemical immunosensor for rapid and sensitive detection of mycotoxins fumonisin B1 and deoxynivalenol. Electrochimica Acta, 213, 89-97.

Ma, Y., Jiang, L., Mei, Y., Song, R., Tian, D., Huang, H. (2013). Colorimetric sensing strategy for mercury(II) and melamine utilizing cysteamine-modified gold nanoparticles. Analyst, 138, 5338-5343.

Miller, J. N., Miller, J. C. (2015). Statistics and Chemometrics for Analytical Chemistry. 6th ed., Pearson Education, UK.

Ndube, N., van der Westhuizen, L., Green, I. R., Shephard, G. S. (2011). HPLC determination of fumonisin mycotoxins in maize: A comparative study of naphthalene-2,3-dicarboxaldehyde and o-phthaldialdehyde derivatization reagents for fluorescence and diode array detection. Journal of Chromatography B: Analytical Technologies in the Biomedical and Life Sciences, 879(23), 2239-2243.

NGFA U.S. (2011). FDA Mycotoxin Regulatory Guidance. A Guide for Grain Elevators, Feed Manufacturers, Grain Processors and Exporters, 9.

Oliva, J. M., Ríos De La Rosa, J. M., Sayagués, M. J., Sánchez-Alcázar, J. A., Merkling, P. J., Zaderenko, A. P. (2018). Solvent-assisted in situ synthesis of cysteamine-capped silver nanoparticles. Advances in Natural Sciences: Nanoscience and Nanotechnology, 9(1), 1-10

Peiris, S., Mcmurtrie, J., Zhu, H. (2015). Emerging processes for green organic synthesis. Catalysis Science & Technology, 6, 320-338.

Plaisen, S., Cheewasedtham, W., Rujiralai. T. (2018). Robust colorimetric detection based on the anti-aggregation of gold nanoparticles for bromide in rice samples. RSC Advances, 8, 21566-21576.

Polte, J. (2015). Fundamental growth principles of colloidal metal nanoparticles - a new perspective. CrystEngComm, 17, 6809-6830.

Rashid, R., Murtaza, G., Zahra, A. (2014). Gold nanoparticles: Synthesis and applications in drug. Tropical Journal of Pharmaceutical Research, 13(7), 1169-1177.

Sabela, M., Balme, S., Bechelany, M., Janot, J., Bisetty, K. (2017). A Review of Gold and Silver Nanoparticle-Based Colorimetric Sensing Assays. Advanced Engineering Materials, 19(12), 1-24.

Sharma, A., Matharu, Z., Sumana, G., Solanki, P. R., Kim, C. G., Malhotra, B. D. (2010). Antibody immobilized cysteamine functionalized-gold nanoparticles for a flatoxin detection. Thin Solid Films, 519(3), 1213-1218.

Sharma, V. K., Yngard, R. A., Lin, Y. (2009). Silver nanoparticles: Green synthesis and their antimicrobial activities. Advances in Colloid and Interface Science, 145(1-2), 83-96.

Sheng, Y., Jiang, W., De Saeger, S., Shen, J., Zhang, S., Wang, Z. (2012). Development of a sensitive enzyme-linked immunosorbent assay for the detection of fumonisin B1 in maize. Toxicon, 60(7), 1245-1250.

Sliem, M. A., Ebeid, E. M., Harith, M. A. (2007). Selective colorimetric detection of viral DNA sequence of hepatitis C virus genotype-4 genetic material using gold nanoparticles. Journal of Biomedical Nanotechnology, 3(4), 360-366.

Souri, E., Kaboodari, A., Adib, N., Amanlou, M. (2013). A New extractive spectrophotometric method for determination of rizatriptan dosage forms using bromocresol green. Journal of Pharmaceutical Sciences, 21(1), 1-6.

Subara, D., Jaswir, I. (2018). Gold nanoparticles: Synthesis and application for Halal authentication in meat and meat products. International Journal on Advanced Science, Engineering and Information Technology, 8, 1633-1641.

Swanglap, P. (2016). Photonics properties of gold and silver nanoparticles. Veridian E-Journal, Science and Technology Silpakorn University, 3, 117-127.

Tangmunkhong, P., Jala, P., Learstsang, W., Laopiem, S. (2008). A survey of fumonisinc contamination in corn produced for feedstuff in Thailand, https://kukr.lib.ku.ac.th/db/index.php?/kukr/search_detail/result/10879. accessed 21.01.2019.

Tansakul, N., Jala, P., Laopiem, S. (2013). Co-occurrence of five fusarium toxins in corn-dried distiller's Grains with Solubles in Thailand and comparison of ELISA and LC-MS/MS for fumonisin analysis. Mycotoxin Research, 29(4), 255-260.

Yoshizawa, T., Yamashita, A., Chokethaworn, N. (1996). Occurrence of fumonisins and aflatoxins in corn from Thailand. Food Additives and Contaminants, 13(2), 37-41.

Thacker (2004). Alkaline hydrolysis. Chapter 6 in Carcass Disposal: A Comprehensive Review. National Agricultural Biosecurity Center Consortium. USDA APHIS Cooperative Agreement Project, Carcass Disposal Working Group.

Thakur, R. A., Smith, J. S. (1996). Determination of fumonisins B1 and B2 and their major hydrolysis products in corn, feed, and meat, using HPLC. Journal of Agricultural and Food Chemistry, 44(4), 1047-1052.

Thompson, E. M. (2008). Standard additions: Myth and reality. Analyst, 133(8), 992-997.

Turner, N. W., Subrahmanyam, S., Piletsky, S. A. (2009). Analytical methods for determination of mycotoxins: A review. Analytica Chimica Acta, 632(2), 168-180.

Visconti, A., Doko, M. B., Bottalico, C., Schurer, B., Boenke, A. (1994). Stability of fumonisins (FB1 and FB2) in solution. Food Additives and Contaminants, 11(4), 427-431.

Voss, K. A., Smith, G. W., Haschek, W. M. (2007). Fumonisins: Toxicokinetics, mechanism of action and toxicity. Animal Feed Science and Technology, 137(3-4), 299-325.

Wang, A., Guo, H., Zhang, M., Zhou, D. (2013). Sensitive and selective colorimetric detection of cadmium (II) using gold nanoparticles modified with 4-amino-3-hydrazino-5-mercapto-1,2,4-triazole. Microchimica Acta, 180, 1051-1057.

Wang, Y., He, C., Zheng, H., Zhang, H. (2012). Characterization and comparison of fumonisin B1-protein conjugates by six methods. International Journal of Molecular Sciences, 13, 84-96.

Willets, K. A., Van Duyne, R.P. (2007). Localized surface plasmon resonance spectroscopy and sensing. Annual Review of Physical Chemistry, 58(1), 267-297

Yamashita, A., Yoshizawa, T., Aiura, Y., Sanchez, P. C., Dizon, E. I., Arim, R. H., Arim, R. H. (2014). Fusarium mycotoxins (fumonisins, nivalenol, and zearalenone) and aflatoxins in corn from Southeast Asia. Journal Bioscience. Biotechnology, and Biochemistr, 59, 8451.

Yazar, S., Omurtag, G. Z. (2008). Fumonisins, trichothecenes and zearalenone in cereals. International Journal of Molecular Sciences, 9(11), 2062-2090.

Young, M. S., Tran, K. (2017). Oasis PRiME HLB cartridges and DisQuE QuEChERS products for UPLC-MS/MS mycotoxin analysis in cereal grains. Waters, 1-3.

Zhang, M., Liu, Y. Q., Ye, B. (2011). Colorimetric assay for sulfate using positively-charged gold nanoparticles and its application for real-time monitoring of redox process. Analyst, 136(21), 4558-4562.

Zhou, W., Yang, S., Wang, P. G. (2017). Matrix effects and application of matrix effect factor. Bioanalysis, 9, 1839-1844.

Zhou, Y., Dong, H., Liu, L., Li, M., Xiao, K., Xu, M. (2014). Selective and sensitive colorimetric sensor of mercury(II) based on gold nanoparticles and 4-mercapto phenylboronic acid. Sensors and Actuators: B. Chemical, 196, 106-111.

Zöllner, P., Mayer-Helm, B. (2006). Trace mycotoxin analysis in complex biological and food matrices by liquid chromatography-atmospheric pressure ionisation mass spectrometry. Journal of Chromatography A, 1136(2), 123-169.

VITAE

Name Miss Thaksinan Chotchuang

Student ID 5910220033

Educational Attainment

Degree	Name of Institution	Year of Graduation
Bachelor of Science (Chemistry)	Prince of Songkla University	2016

Scholarship Awards during Enrolment

The Research Assistantship (Contract No. 1-2559-02-002), Faculty of Science, Prince of Songkla University

The Center of Excellence for Innovation in Chemistry (PERCH-CIC), The Office of the Higher Education Commission, Ministry of Education (OHEC)

The Graduate School, Prince of Songkla University

List of Poster presentations and Publication

Poster presentations

Chotchuang, T., Rujiralai, T., Cheewasedtham, W. "Rapid colorimetric method for detection of fumonisin B1 in corn samples" The PERCH-CIC Congress X, July 4-7, 2018, Jomtien Palm Beach Hotel, Pattaya, Thailand.

Chotchuang, T., Jayeoye, T., Cheewasedtham, W., Rujiralai, T. "Simple and selective colorimetric detection for fumonisin B1 in corn samples" The 6th Thailand International Nanotechnology Conference (Nanothailand2018), December 12-14, 2018, the Thailand Science Park Convention Center, Pathumthani, Thailand.